EXPERIMENTAL AND NUMERICAL INVESTIGATION OF COMBINED HEAT TRANSFER ENHANCEMENT TECHNIQUE IN GAS-HEATED CHANNELS

DMITRI NESHUMAYEV

Faculty of Mechanical Engineering
Thermal Engineering Department
TALLINN UNIVERSITY OF TECHNOLOGY

Dissertation was accepted for the defence of the degree of Doctor of Philosophy in Engineering on May 16, 2005.

Supervisors:
Cand. of Tech. Sc., Prof. T. Tiikma, Faculty of Mechanical Engineering
DSc I. Klevtsov, Faculty of Mechanical Engineering

Opponents:
Dr. habil., Prof. Jurgis Vilemas, Lithuanian Energy Institute, Lithuania
Dr., Prof. Reijo Karvinen, Tampere University of Technology, Finland

Commencement: September 5, 2005

Declaration
Hereby I declare that this doctoral thesis, my original investigation and achievement, submitted for the doctoral degree at Tallinn University of Technology has not been submitted for any degree or examination.

EXPERIMENTAL AND NUMERICAL INVESTIGATION OF COMBINED HEAT TRANSFER ENHANCEMENT TECHNIQUE IN GAS-HEATED CHANNELS

Dmitri Neshumayev
Thermal Engineering Department
Tallinn University of Technology
Kopli 116, 11712, Tallinn
Estonia

Abstract

The given thesis is dedicated to the experimental and numerical investigations of the combined heat transfer enhancement technique and the device, which is based on this technique and proposed for the heat transfer augmentation in the gas-heated channels. The given device is the twisted tape with the oppositely coiled spiral tape installed above it. The geometrical characteristics of the investigated inserts were the following: the relative twist ratio of the internal twisted tape $y \approx 2 - 4$, the relative height of the external tape $e/D \approx 0.07 - 0.2$ and the relative pitch of a spiral coiling of the external tape $h/D \approx 1 - 2$.

The experimental study of the heat transfer was performed directly in the convective part of two fire-tube boilers of different design that had both the vertical and horizontal arrangement of the flue tubes. The combustion products of the applied fuels, a light oil fuel and wood pellets, respectively, were used as the working fluid. The Reynolds number varied within the range of $2500 - 5500$. The pressure drop characteristics of the inserts were studied by means of the specially designed and constructed experimental set-up at the isothermal condition at the same Reynolds numbers. In order to validate the experimental technique, the separate experiments were carried out with the smooth pipe, the tubes with the inserted straight and the twisted-tape inserts.

The 3D numerical simulation has been carried out for the fully developed flow using the periodic boundary conditions by means of the RNG $\kappa-\varepsilon$ turbulence model with the applying of the FLUENT CFD code. The obtained numerical results were compared with the data got during the experimental program of this study.

The significant increase of the heat transfer coefficients has been revealed as compared with the pure twisted tape or the pure enhanced tubes.
The method for the prediction of the heat transfer coefficients and the friction factors is additionally proposed for the fully developed turbulent flow regime.

Keywords: Heat transfer augmentation, straight and twisted tapes, combined heat transfer enhancement

SOOJUSÜLEKANDE KOMBINEERITUD INTENSIIVISTUSSEADMETE EKSPERIMENTAALNE JA NUMBRILINE UURING GAASIGA KUUMUTATAVATES KANALITES

Dmitri Nešumajev
Tallinna Tehnikaülikool
Soojustehnika instituut
Kopli 116, 11712, Tallinn

Kokkuvõte

Käesolevas töös uuritakse katseliselt ja numbriliselt kombineeritud seadet soojusülekande suurendamiseks, antud konkreetsel juhul seadet soojusülekande suurendamiseks gaasiga jahutatavates kanalites. Seade kujutab endast spiraalset linti, mille peale on keeratud veel teisesuunalise spiraaliga lint. Lintide geomeetrilised parameetrid olid järgmised: seesmise spiraali suhteline samm $y \approx 2 - 4$, välimise lindi spiraali suhteline kõrgus $e/D \approx 0.7 - 0.2$, välimise spiraali suhteline samm $h/D \approx 1 - 2$.

Soojusülekande eksperimentaalne uurimine toimus kahe erineva konstruktsiooniga leektoru katla konvektiivses osas, kus torud asetsesid nii vertikaalselt kui ka horisontaalselt. Töökeskkonnaks osutusid seega kateldes kasutatavate kütuste, kerge kütteõli ja kabulad, põlemissaadused. Reynoldsi arvud kõikusid piirides $\sim 2500 - 5500$. Seadme hüdraulilist takistust uuriti isotermiliselt eraldi stendis samade Reynoldsi arvude juures. Katsemetoodika kontrolliks tehti võrdluskatseid siledas torus ning sissepandud tasapinnaliste ja spiraalsete lintidega torudes.

Numbriliselt modelleeriti (3D) voolamist RNG k-ε turbulentsi mudeliga FLUENT CFD programme abiga täielikult stabiliseerunud voolamise jaoks (perioodilised ääretingimused) ainult ühte tüüpi kombineeritud turbulisaatoris. Numbrilise modelleerimise tulemused ja katsetulemused langesid hästi kokku. Kombineeritud seadme kasutamine tõstab üldjuhul soojusülekandetegurit märgatavalt, võrreldes ainult ribitatud pinnaga või ainult ühekordse spiraaliga varustatud toruga.

Ühtlasi esitatakse selles töös meetod soojusülekandetegurite ja hüdraulilise takistuse arvutamiseks täielikult stabiliseerunud turbulentsele voolamisele.

FORMATTING OF THE THESIS

The given thesis may be divided by the matter into two main parts – the experimental investigation and the numerical simulation. The experimental part included the study of the thermalhydraulic characteristics of inserts of two different determined sets of the geometrical parameters, which was performed on two fire-tube boilers, and the experimental study of the four additional inserts with different geometrical parameters performed on the same experimental set-ups and of the friction factors of insert, which was carried out in the isothermal conditions. The first experimental part of the thesis is based mainly on the publications, that completely cover the experimental study of the thermalhydraulic characteristics of inserts in two fire-tube boilers. At the same time, the contents of these papers is presented in the revised form because of the better understanding of the studied phenomena by the author of the given thesis. The remaining part of the thesis, which summaries the experiments with the additional geometrical parameters of inserts, the study of friction factor characteristics in the isothermal conditions and the numerical simulation have not been published until now, and so it is presented in more detailed form.

The publications that cover almost completely the experimental study of the thermalhydraulic characteristics of inserts are the following:

I. Neshumayev D., Ots A., Laid J., Tiikma T. *Heat transfer augmentation and pressure drop of turbulator inserts in gas-heated channels* pp. 565-572. In: Advances of Heat Transfer Engineering (Proc. of 4th BHTC, Kaunas, Aug. 25-27, 2003). Ed. by B. Sunden and J. Vilemas.

II. Dmitri Neshumayev, Arvo Ots, Jaan Laid, Toomas Tiikma. Experimental investigation of various turbulator inserts in gas-heated channels. Experimental Thermal and Fluid Science, 28/8 pp.877-886, 2004

III. Boiler tube flue turbulator, Utility model certificate of Estonian patent office, no U200300057 (Kasuliku mudeli tunnistus nr. 00441 U1 *Katla-suitsutoru turbulaator* (51) Int.CL F28B 13/12; F23B 37/06. autorid: J. Laid, P. Must, D. Neshumajev, A. Ots, T. Tiikma.)

Contributions by Dmitri Neshumayev

Papers I, II: The author has suggested the methodology of the experimental measurement procedure for the heat transfer coefficients. The author has designed and made the required devices for the measurements of temperature and other determining parameters. The author has developed additionally the software support for the automation of the data acquisition of some determining parameters. The author has elaborated the software support for the processing of the experimental data and performed the data reduction. The author took part directly in the running of the experiments

and discussion of the obtained data. The author has written the presented joint papers.

Paper III: The author is the principal developer of the given technique

Unpublished material: The author has suggested the methodology of the experimental procedure concerning the measurements of the friction factor coefficients in the isothermal conditions. The author has designed and built the experimental set-up. The author has performed the experiments and the appropriate experimental data processing. The numerical simulation has been carried out completely by the author. The author has proposed the method of the correlation for prediction of the heat transfer and friction factors for the combined inserts.

The subject of the defence:

The subject of the defence is the combined heat transfer augmentation technique, the results of the experimental investigation of the mean heat transfer of the proposed insert for the flue gas heated channels, and the appropriate experimental procedure of measurements of the specified parameters, the experimental results of the hydraulic characteristics of inserts and appropriate experimental set-up and the technique of the experiments, the results of the numerical simulation including the general flow pattern, the local distributions of the heat transfer coefficients and wall shear stress on the tube wall, the method of the correlation for the prediction of the heat transfer coefficients and friction factors of the combined inserts.

Scientific novelty of the obtained results:

The experimental and the numerical data of the mean and the local heat transfer coefficients and the friction factors concerning the little-studied combined heat transfer augmentation technique, which uses the twisted tape, have been obtained for the laminar and the transition flow regimes at the cooling conditions of gas. Based on the numerical simulation, the method for the prediction of the heat transfer coefficients and friction factors has been proposed for the fully developed turbulent flow regime.

SCOPE OF THE THESIS

The thesis consists of introduction, the literature review containing the concise description of the studies, which are available on the given subject, five chapters containing the description of the experimental and numerical methods, the presentation and discussion of results, the states of the correlation development, and conclusion. The list of the cited literature is presented at the end of the thesis. The more detailed description of each part is presented below.

Chapter 1 (Literature Review) surveys the published results concerning the heat transfer augmentation technique in channels with the combined applying of the twisted tape and the surface ribbing (or the three-dimensional surface roughness or the local axial vane swirler). In spite of the relatively high efficiency of the technique reported by various authors, there are only few publications on the given subject.

Chapter 2 (Experimental Set-up) gives the concise description of the applied experimental apparatus, namely two fire-tube boilers of different design, as well as the specially designed and constructed experimental set-up. The first two experimental apparatus were mainly used for study of the thermal characteristics of the proposed device, as well as the experimental investigation of the hydraulic characteristics of the considered inserts. Specially designed and constructed, the third experimental set-up was used only for study of the hydraulic characteristics of inserts at the isothermal conditions. The given chapter contains also the analysis of the state of the art of knowledge for the effect of variability of the thermal properties of the gas flow at the cooling condition, which was carried out in order to adequately interpret the obtained experimental data. The methods of the raw experimental data processing and the analysis of the experimental uncertainties are also presented in this chapter.

Chapter 3 (Numerical Calculation) gives the concise description of technique of the numerical modelling applied in the given thesis. It includes the problem statement, the mathematical formulation with the description of the used turbulence models and the boundary conditions, as well as the procedure of modelling. The numerical solving of the differential equations was carried out with the help of the available commercial CFD code FLUENT 6.1.22, and the geometry and the grid of the computational domain were prepared by the GAMBIT 2.1.6 software.

Chapter 4 (Results and Discussion) presents the main results obtained both by the numerical simulation and the experiments. The given chapter is divided into several parts. The first part discusses the thermalhydrualic characteristics of the smooth pipe, the straight and twisted tapes, including the radiation effects, that occur between the surfaces of the insert and the tube. The comparison of the obtained results, which showed a good agreement with the data by other authors and indicated the reliability of the experimental data, is also presented in this chapter. The second part of the given chapter summarizes the results of the mean convective heat transfer and the pressure drop of the combined turbulators obtained during both the experiments and the numerical simulation. Here the comparison with the rare studies, which are close to the

proposed method of the heat transfer augmentation described in the first chapter of the thesis, is also carried out. The third part of the given chapter involves the discussion of the data obtained for the local convective heat transfer, the wall shear stress and the flow pattern derived through the 3D numerical simulation, which was performed in the framework of the given study.

Chapter 5 (Some Considerations For Correlation Development and Further Works) states briefly the analysis, which has been carried out by the author for the development of the correlation, which allows to predict the convective heat transfer coefficients and the friction factors for the fully developed turbulent flow regime. The main conclusions are drawn in the final part.

The thesis is supplied by the list of the cited literature, which is presented at the end of the thesis.

PREFACE

I would like to express my gratitude to everyone who has in one way or another contributed to this work.

I would like to express my deepest gratitude to the scientific supervisors, Dr. H. Käär and Dr. T. Tiikma, who unfortunately are no more among us, and also Dr. I. Klevtsov, for their excellent guidance, valuable advices, friendship and support for solving problems connected not merely with my scientific effort.

I owe my gratitude to my colleagues and collaborators from the Thermal Engineering Department and the Laboratory of Multiphase Media Physics, TUT, for their valuable advices and useful discussion of the obtained results.

I am also grateful to MSc S. Tisler for correcting the English.

I wish to express my thankful appreciation to my family and friends for their continuous support, understanding and encouragement, which cannot be overemphasized.

Table of Contents

NOMENCLATURE

Roman symbols

c_p specific heat at constant pressure, J/(kg K)

c_t correction factor related with the thermal entrance effect, Eq. (3).

c_x correction factor related with the pipe length $(=(1+(L/D)^{-2/3}))$, (dimensionless)

D tube inside diameter, m

e rib height, m

f_{Darcy} Darcy friction factor $(= 8\tau_w/(\rho u_m^2))$, (dimensionless)

f, C_f Fanning friction factor $(= f_{Darcy}/4)$, (dimensionless)

g gravitational acceleration, m/s^2

Gr Grashof number

Gz Graetz number $(= \text{Re}\,\text{Pr}\,D/L)$

H 180 deg twist pitch, m

K_t dimensionless turbulence scale factor

L tube length, m

$\dot{m}$ mass flow rate, kg/s

Nu Nusselt number

p rib pitch, m

Pr Prandtl number

Pr_t turbulent Prandtl number

q_{TURB}^c heat flux (by convection) between gas medium and turbulator, W/m^2

q_{TURB}^R heat flux (by radiation) between turbulator surface and tube surface, W/m^2

Ra_{LM} Rayleigh number based on the logarithmic-mean temperature difference

Re Reynolds number

Re_{sw} Reynolds number based on a swirl velocity

St Stanton number

Sw dimensionless swirl parameter $(= \text{Re}_{sw}/\sqrt{y})$, (dimensionless)

T temperature, K

Δt temperature difference between the wall and bulk fluid temperatures, K

U_i mean velocity component, m/s

U_τ shear velocity, m/s

U^+ dimensionless velocity (U/U_τ)

x distance from the tube edge, m

y twist ratio, H/D or normal distance to the wall, m

y^+ dimensionless distance from the surface $(=yU_\tau/\nu)$

Greek symbols

α heat transfer coefficient, W/(m^2 K)

β	coefficient of an isobaric thermal expansion, K^{-1}; or helix angle, deg
δ	twisted tape thickness, m
δ_{ij}	Kronecker delta ($\delta_{ij}=1$ if i=j and $\delta_{ij}=0$ if i≠j)
λ	thermal conductivity, W/(m K)
μ	fluid dynamic viscosity, kg/(m s)
θ	temperature ratio, T_w/T_b
ρ	fluid density, kg/m^3

Subscripts

b	bulk fluid temperature measure
F	forced convection value
m	mean value
M,O	mixed convection (opposing) value
N	natural convection value
w	tube wall measure
0	isothermal condition value
360°	deg twist
h	based on hydraulical diameter

INTRODUCTION

As is well known, the fuel resources of our planet are very scanty. Therefore, there is a continuous growth of a fuel cost, and so at present more and more attempts are made to increase the efficiency of the power equipment, which is applied for various industrial applications. One particular case of the increasing of the efficiency is the heat transfer augmentation in channels of the heat-exchange equipment.

The first attempts of the heat transfer intensification were made more than a century ago, and to date there are many techniques to achieve this purpose. These techniques can be both passive, i.e. not requiring the direct input of the external power, and active, i.e. applying an addition of the external power. Now about 400 papers and technical reports on the given matter are published every year (Bergles, 2002).

As it was supposed before, under the hydraulic theory of heat transfer based on Reynolds' analogy, which determines a similarity between the processes of heat and momentum transfer and is expressed analytically by the following formula:

$$\text{St} = \frac{1}{2}C_f,\qquad(1)$$

the heat transfer can be increased only by the neglecting of rising of the friction factor.

However, the experimental and theoretical investigations, carried out at the second half of the last century, have shown that a certain impact applied in the necessary direction for a flow structure could result in the violation of Reynolds' analogy. The desired flow structure modification can be achieved by the applying of various devices, such as the spherical dimples on a surface (see, for example, Gachechiladze *et al.* (1988)), rough surfaces (see for example Pedišius & Šlančiauskas, (1995), Kalinin *et al.* (1990), and other works) and longitudinal microribbing[1] (Riblets) (see, for example, Neshumajev *et al.* (1999), Katoh *et al.* (2000)). These devices have to impact on a near-wall flow, since the maximum thermal resistance is concentrated just in a wall boundary layer. The mechanism of the heat transfer intensification by the given techniques consists in a creation of the ordered vortex structures near the wall, a flow separation zone and etc.

In addition to the above mentioned passive techniques of the heat transfer augmentation, there are another ones, which are less effective and, as a rule, lie in an enlargement of the heat-transfer surface area.

It is known, that the combination of two or more single enhancement techniques may result in more significant effect, as compared with the applying of individual methods. The given devices are denoted as the combined, and the corresponding process of intensification is called as the third generation enhancement (Bergles, 2002).

---

[1] Though, the attribution of riblets to the given class of the heat transfer intensification surfaces is disputable.

The given thesis is dedicated to the experimental and numerical investigations of the simultaneous applying of the twisted tape and spiral ribbing, which were combined into the single device (see **Fig. 1**). This device was developed and offered for the heat transfer augmentation in a convective part of two different fire-tube boilers, which were under design at that time (see the utility model), by the research team of TUT TED[2] jointly with the author of the given thesis.
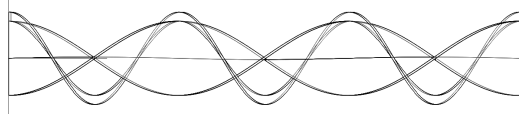
Fig. 1. Combined heat transfer device

Further, the brief description of state of the art, concerning individually the twisted tape, the rough surface and the combined technique, which is close to the method proposed in the given thesis, will be presented. It should be noted the scarcity of the investigations (no more than ten) which regards the combined enhancement of the heat transfer. Here, the single-phase flow conditions are under consideration, and one unit in the compound enhancement techniques is the twisted tape.

Rib roughness (enhanced tubes)
As mentioned above, one of the most effective methods of intensification of the convective heat transfer may be the turbulizing protuberances, which are periodically located on a heat-transfer surface and disturb the viscous sublayer of the near-wall turbulent flow structure, where the thermal resistance is the maximum[3]. Numerous investigations, both experimental and numerical, dealt with the study of the mechanism of intensification of the heat transfer by applying these techniques. Let us consider the results of some recent investigations, which seem to be the most particular in respect to the revealing of the entity of the mechanism of intensification of the heat transfer, including a flow pattern, distribution of the local convective heat transfer coefficient, the integral convective heat transfer coefficient and other determining factors.

The recent numerical investigations by Nagano *et al.* (2004) and Cui *et al.* (2003) of a turbulent flow in a flat channel with periodically located transverse ribs of the rectangular cross-section, by applying the DNS and LES methods, respectively, have revealed the flow pattern, generally depended on the relative pitch of the ribs arrangement, that confirmed the results of the earlier researches. These studies were conducted[4] at $Re_{\tau 0} = 150$ and $Re = 10000$,

---

[2] TUT TED – Tallinn University of Technology Thermal Engineering Department.

[3] It is known, that for gases ($Pr \approx 0.7$) the thermal resistance is distributed as follows: about 35 % occurs in a viscous sublayer, roughly 50 % takes place in a buffer zone and about 15 % is in a turbulent core. For oils ($Pr = 20$) the main part of the thermal resistance is concentrated in a viscous sublayer (about 99 %) (Migay, (1987))

[4] In the calculation of $Re_{\tau 0}$ the friction velocity is used as the characteristic and the half of width of the channel is applied as the linear dimension. In the second paper the mean fluid velocity and the half of width of the channel are used as the characteristic parameters for calculation of the Re number.

17

respectively. It was obtained that sufficiently close-packed compact arrangement of ribs, when the relative pitch *p/e* is less than 4 (the so-called d-type of roughness), resulted in formation of the 3D cellular vortex in a cavity, which locates between two adjacent ribs, and made the streamlines, located above the upper surface of the rib, to be parallel to it.

When the relative pitch *p/e* was about 4 (the so-called intermediate type of roughness), a vortex was also generated between the ribs, and it filled all the area between two adjacent ribs. Besides, a small counter-rotating vortex was generated on the near lower part of the leeward surface of the rib. The streamlines above the upper plane of the rib surface remained also practically parallel to it.

At *p/e* > 4 (the so-called k-type of roughness) four vortex zones were revealed. The first one, which was a small separation zone arisen on the upper plane of the rib, was caused by the presence of a sharp edge on the frontal surface, which affected an incident flow, that come from the preceding interrib space. The second zone, which was the most considerable separated flow, arose behind the rib, and a small counter-rotating vortex formed near the base of this rib (the leeward side). Further, the area of redevelopment region (the relaxation zone) arose behind the reattachment point of the main separated flow, that resulted in the fourth vortex near the front upstream rib. It was found that the relative sizes of the considered vortexes did not depend on Re.

These numerical investigations have shown that the increase of the rib height intensified a turbulence generation in the middle of enclosure in the interrib space. This conditioned the increasing of the turbulent stresses and a turbulence kinetic energy, and these fluctuations affected a flow above a centerline of a flat channel, that assumed the presence of a large-scale interaction between a flow near the ribs and an external flow. The turbulence generation occurred in the interrib space was caused mainly by the contribution of terms of a turbulent and pressure diffusion, i.e. a turbulent transport.

Nagano *et al.* (2004) also have shown that the turbulent Prandtl number Pr_t was not constant near the ribbed surface, that indicated a lack of analogy between the turbulent transfer of heat and momentum. For example, in the middle of an enclosure between two adjacent ribs, Pr_t reduced at first, and then it rose again with the increase of the normal distance from a wall.

Hishida (1996) experimentally investigated a local convective heat transfer in the domain of the transverse ribbed surface with the rectangular ribs in an air flat channel flow for both types of roughness (k-type and d-type). The Re numbers varied over the range $3 \cdot 10^3 - 10^5$. As it was shown above, the flow pattern in the enclosure of two adjacent ribs is generally determined by the ratio between the rib pitch and the rib height. It is reasonable that the distribution of the local heat transfer coefficient over the rib surface and within the interrib space is also determined by the relative pitch *p/e*.

When *p/e* is more than roughly 10, the distribution of the Nu number on the base surface, between two adjacent ribs, has a maximum in a reattachment zone of a separated flow, and the further decreasing of Nu from this zone, both

upstream and downstream (relaxation zone), will occur. Also, there is a second maximum in the given distribution of Nu, which locates near the frontal surface of the downstream rib. When *p/e* is less than 5, the distribution of Nu on the base surface in the interrib space has a maximum, that is close to the frontal surface of a downstream rib, and it tends to decrease in the upstream direction from this point.

The distribution curve of Nu on the frontal surface of a rib monotonously descends from the point of the maximum located at the top of the given surface. The distribution curve of the local Nu on the upper surface of a rib, depending on the ratio *p/e* and/or the Re numbers, has either the monotonous decrease in the streamwise direction from the frontal vertex or passes through a maximum, that locates in a central part of the upper surface of a rib. Hishida (1996) have shown that the latter distribution of the local Nu took place at large *p/e*, that agrees with a flow pattern described earlier, and/or the Re number.

In recent investigation by Ravigururajan & Bergles (1996), an attempt to systematize the extensive experimental data, obtained for the friction factors and convective heat transfer in the rib-roughened channels, was made by applying of the statistical methods. The derivation of resultant equations was based on the data, obtained by seventeen experimental researches that covered the following range of the determining parameters: $0.01 \leq e/D \leq 0.2$, $0.1 \leq p/D \leq 7.0$, $0.3 \leq \alpha/90 \leq 1.0$, $5000 \leq \mathrm{Re} \leq 25000$ and $0.66 \leq \mathrm{Pr} \leq 37.6$. The heat flux direction was from a wall to a working fluid (the heating condition) for all the considered investigations. The authors have derived the following equations for the friction factor and convective heat transfer, respectively, by entering also the asymptote behaviour for the smooth pipe:

$$
f_a/f_s = \left\{ 1 + \left[\begin{array}{l} 29.1\,\mathrm{Re}^{(0.67-0.06p/D-0.49\alpha/90)} (e/D)^{(1.37-0.157p/D)} \times \\ \times (p/D)^{(-1.66\times E-6\,\mathrm{Re}-0.33\alpha/90)} \times \\ \times (\alpha/90)^{(4.59+4.11\times E-6\,\mathrm{Re}-0.15p/D)} (1+2.94\sin\beta/n) \end{array} \right]^{15/16} \right\}^{16/15} , \quad (2)
$$

$$
\mathrm{Nu}_a/\mathrm{Nu}_s = \left\{ 1 + \left[2.64\,\mathrm{Re}^{0.036} (e/D)^{0.212} (p/D)^{-0.21} (\alpha/90)^{0.29} (\mathrm{Pr})^{0.024} \right]^7 \right\}^{1/7} , \quad (3)
$$

where f_s and Nu_s are taken for the smooth pipe condition based on the equations by Filonenko and Petukhov-Popov, respectively.

The last term of the right part of the first equation takes into account the streamlining effects of a rib profile. Here *n* is a number of the sharp corners in the roughness element in the facing flow. One can see also that the equation for the convective heat transfer does not contain the similar parameter for the account of a rib profile, due to the absence of a noticeable influence of the last one on the convective heat transfer.

Ravigururajan & Bergles (1996) have carried out also the experimental investigations in order to check the correlations (2) and (3). They arranged both the heating condition, applying water as the working fluid, and the cooling condition using air. The obtained experimental data were in good agreement with the derived equations. In addition, Ravigururajan & Bergles (1996) have shown that the influence of a rib height on the heat transfer dominated over such determining factors, as the rib pitch or the Re number. The greater values of the rib height resulted in more fast increase of the friction factor as compared to the convective heat transfer. The pitch of a roughness element had the similar effect on the friction factor and the convective heat transfer.

Besides, the authors got the unexpected effect of a character of influence of the ribbing helix angle on the friction factor f. It was obtained that f slightly increased with the growth of the helix angle up to 20°, then strong increase of f up to ~70° occurred and, further, the stabilization of f took place. The authors supposed that such fact was due to the increase of predominance of effect of the cross flow over the rotational flow, that occurred at the increase of the helix angle. It was also found that the influence of the Pr number on the heat transfer augmentation was insignificant, that confirmed the earlier results obtained by other authors.

Usually, the experimental data on the convective heat transfer and friction factors in channels, having the considered type of the regular roughness, are tried to generalize extending the interpretation of study by Nikuradse and Dipprey & Sabersky (1962) on a random sand-grain roughness and analogy between the momentum and heat transfer roughness functions, respectively. Then, the dimensionless velocity profile can be expressed as follows:

$$U^+ = 2.5\ln(y/e) + R(e^+),$$ (4)

where the factor 2.5 in the first term of the right part is the inverse value of the universal constant in the mixing length of Prandtl's mixing length model, and $R(e^+)$ is the momentum transfer roughness function.

Dipprey & Sabersky (1962) have shown that for the turbulent number $Pr_t = 1$ the temperature distribution in the near-wall areas was similar to the velocity distribution:

$$\upsilon^+ = 2.5\ln(y/e) + G(e^+, Pr),$$ (5)

where $G(e^+, Pr)$ is the heat transfer roughness function.

Generally, three modes of roughness can be distinguished:
1. the hydraulically smooth surface at $e^+ \leq 5$;
2. the transient mode, when the elements of roughness partially are beyond the laminar sublayer at $5 \leq e^+ \leq 70$;
3. the mode of the full manifestation of roughness at $e^+ > 70$.

Earlier investigations were mainly aimed at the searching or developing of the correlations for the momentum and heat transfer roughness functions.

20

However, some authors inclined to consider that such method of analogy was not completely correct, since, as some researches have shown, the turbulent Prandtl number $\mathrm{Pr_t}$ varied over the wide range for the given roughness type (see, for example, Nagano *et al.* (2004)). Thus, there is not any suitable scaling law for the reduction of the developing hydrodynamical and thermal profiles, occurred near the surface with such kind of roughness, to a single function.

Twisted-tape insert

The twisted tape is one of the effective heat transfer enhancement techniques, which is applied mainly for the heat transfer intensification in the fire-tube boilers, and is known for a long time (Junkhan *et al.* (1985)). Here a plenty of the experimental and numerical researches have been carried out to date, but, nevertheless, the twisted tape also remains the subject of inquiry nowadays.

It is regarded that the main mechanisms, which are responsible for the heat transfer augmentation in case of application of the twisted tape, are the next: the increase of the effective length of a flow path, the secondary fluid motion formation due to the superimposed centrifugal forces in a helically twisting fluid, the increase of a fluid velocity due to the blockage of a tube cross-section as well as the fin effect at the tight installation in a tube (see, for example, Manglik & Bergles, (1993a, b)).

The friction factors and the heat transfer coefficients can be correlated by the dimensionless swirl parameter Sw under the conditions of the fully developed laminar flow in a tube at presence of the twisted tape. The given parameter Sw follows from the balance of forces, that are imposed in a twisted-tape flow, where the centrifugal and inertial forces are balanced by the viscous force (Manglik & Bergles, (1993a, b)). The twist ratio of the twisted tape *y* becomes the determining factor for the fully developed turbulent flow.

Manglik & Bergles (1993a, b) have made an attempt to derive the general correlation of friction factors and heat transfer coefficients, that took into account the free convection, thermal entrance effects and covered all the flow regimes from laminar to turbulent. The derived general correlation for friction factors is as follows:

$$f = \left(f_l^{10} + f_t^{10} \right)^{0.1},\tag{6}$$

where

$$f_l = \frac{15.767}{\mathrm{Re}} \left(1 + 10^{-6} Sw^{2.55} \right)^{1/6} \left(1 + (\pi/2y)^2 \right) \times$$
$$\times \left(\frac{\pi + 2 - 2\delta/D}{\pi - 4\delta/D} \right)^2 \left(\frac{\pi}{\pi - 4\delta/D} \right), \quad \mathrm{Re} \to 0 \tag{7}$$

and

$$f_t = \frac{0.0791}{\mathrm{Re}^{0.25}} \left(\frac{\pi}{\pi - 4\delta/D} \right)^{1.75} \left(\frac{\pi + 2 - 2\delta/D}{\pi - 4\delta/D} \right)^{1.25} \left(1 + \frac{2.752}{y^{1.29}} \right), \quad \mathrm{Re} \to \infty. \tag{8}$$

21

Here the second equation is valid for the pure laminar flow, and the third one is suitable for the pure turbulent flow. These equations use the internal diameter of a tube and the flow velocity, which is calculated by the internal cross-section of a tube, as the determining parameters for the similarity criteria. Later, Manglik *et al.* (2001) have performed the scaling and validation of Sw and these equations for the laminar flow regime and the comparison of them with the data of other researchers. The excellent agreement with the prediction was found, where all the data fell within ±15% interval, and the majority of the data did not exceed the ±10% domain at enough broad range of the determining parameters: $1.5 \le y \le \infty, \ 0 \le \delta/D \le 0.2, \ 0 \le Sw \le 2500$.

Manglik & Bergles (1993a,b) have proposed the following general correlation for the Nu number in the twisted-tape flows:

$$
\begin{cases}
1. \quad \mathrm{Nu}_m = 4.612 \left[\dfrac{\left(1 + 0.0951\,\mathrm{Gz}^{0.894}\right)^{2.5} +}{+\, 6.413 \cdot 10^{-9} \left(Sw\,\mathrm{Pr}^{0.391}\right)^{3.835}} \right]^{0.2}, \quad Sw < 1400; \\[4mm]
2. \quad \mathrm{Nu}_m = \mathrm{Nu}_{y=\infty}\left[1 + 0.769/y\right]; \quad \mathrm{Nu}_{y=\infty} = 0.023\,\mathrm{Re}^{0.8}\,\mathrm{Pr}^{0.4} \times \\[2mm]
\qquad \times \left(\dfrac{\pi}{\pi - 4\,\delta/D}\right)^{0.8} \left(\dfrac{\pi + 2 - 2\,\delta/D}{\pi - 4\,\delta/D}\right)^{0.2}, \quad \mathrm{Re} > 10000; \\[4mm]
3. \quad \text{LINEAR INTERPOLATION}, Sw > 1400 \quad and \quad \mathrm{Re} < 10000.
\end{cases}
\tag{9}
$$

The first correlation in Eq. (9) describes the heat transfer in the laminar flow for $Sw < 1400$, which also takes into account the thermal entrance effects. Here the influence of the free convection is ignored, because of $\mathrm{Gr} < Sw^2$. The second correlation describes the heat transfer of the fully developed turbulent flow for the flow regimes at $\mathrm{Re} > 10000$. The authors recommended to use the linear interpolation between the laminar and turbulent flow regimes for the heat transfer calculation in the transition flow regime ($Sw > 1400; \ \mathrm{Re} < 10000$).

1. LITERATURE REVIEW

There are only some investigations devoted to the study of the combined convective heat transfer phenomenon, where one of the heat transfer enhancement techniques is the twisted tape (the single-phase flow considered here).

The experimental investigation by Bergles *et al.* (1969) seems to be one of the first works, where the research of influence of the combined use of a surface roughness and the twisted tape on the convective heat transfer was carried out. Here the experiments were carried out using water as the working fluid at two directions of a heat flux (the heating and cooling conditions). The correlation for a quantitative assessment of the heat transfer coefficients was experimentally obtained based on the additive technique developed by Lopina & Bergles, (1969). According to this technique, the total heat flux was calculated as the sum of heat fluxes, that correspond to a spiral convection, a centrifugal convection and a fin effects. It was also noted that there was no special duplication in two mechanisms of the arising phenomenon.

Van Rooyen & Kröger (1978) have studied experimentally for the first time the combined application of the twisted tape and the longitudinal ribbing for the laminar flow of oil. The variation range for the Re number, which was determined by the hydraulic diameter, and the Pr number were $50 - 2000$ and $114 - 490$, respectively. These experiments were conducted with the implementing of both heat flux direction schemes (the cooling and heating conditions) and the wall constant temperature boundary condition was realized. Van Rooyen & Kröger (1978) observed the significant increase of the heat transfer after the additional insertion of the twisted tape for $y \approx 2.5$. The maximum obtained value of the augmentation of the heat transfer was in three times greater at the constant pumping power for the heating conditions and in four times greater for the cooling conditions as compared with the smooth tube.

Usui *et al.* (1986) experimentally studied the convective heat transfer of water and $40 - 60$ wt.% aqueous solution of glycerine in the internally grooved rough tube with and without the twisted tape, over the range of the Re number of $2 \cdot 10^3 - 10^5$ and the Pr number $5.4 - 46.6$. The constant heat flux boundary condition on a wall was implemented in the experiments. As a result of the combination of two enhancement techniques, the authors observed the more considerable increase of the heat transfer as compared with a separate application of each type. The largest enhancement of the convective heat transfer was achieved, when the ribbing and the twisted tape were positioned in the opposite direction, and the relative height of ribs *e/D* was about 0.022, that were the maximum values for those experiments. The evaluation of performance of the considered enhancement techniques have shown that at constant pumping power the reduction of the heat transfer surface area could be achieved $70 - 75$ %.

Almost ten years later, Zhang *et al.* (1997) experimentally studied the thermalhydraulical characteristics of the combined use of the axial interrupted ribs having the in-line or staggered arrangement as well as the twisted tape. This

research was conducted using an air as the working fluid at the constant heat flux on a wall. The Re number varied within the range 1700 – 8200. The maximum increase of the heat transfer in case of a tube, having the twisted tape of $y = 3$ and the axial interrupted ribs in the staggered arrangement (the rib height e/D equalled 0.125), was 2.2 – 3.2 times as compared with the smooth tube at the simultaneous increase of the friction factor of 13 – 14 times depending on the Re number. Zhang *et al.* (1997) also have made an attempt to measure the distribution of the local heat transfer coefficient, which was determined as the mean value over a short section of a tube with 38.1 mm length and the internal diameter 25.4 mm. Those measurements have shown that in case of use of the twisted tape only the distribution curve of ratio between the piecewise averaged Nu number and the Nu_0 number for the smooth surface depending on the relative length of a tube, stabilized at x/D $\approx$ 2. When the additional installation of the axial ribs with the staggered arrangement was done, the distribution curve of the ratio Nu/Nu_0 over the relative length of a tube first decreased at x/D $\approx$ 2, then increased passing through its maximum at x/D $\approx$ 4 – 8, and further decreased again. The authors attributed such behaviour to the secondary flow, induced by the rib orientation relative to the swirling flow. The estimation of the heat transfer performance has shown that at the constant pumping power and the heat-transfer surface area, the proposed combination of the enhancement devices allowed to increase the efficiency of the heat transfer ($\left[Nu/Nu_0\right]\big/\left[f/f_0\right]^{1/3}$) as 25 – 40% as compared with the only twisted-tape insertion.

It is worth to notice the work by Liao & Xin (2000), where the experimental research of the thermalhydraulical characteristics of flow with the combined use of a tube, having the internal 3D artificial roughness (the roughness element was the triangular prism) and the twisted tape, was performed. Water, ethylene glycol and a turbine oil (ISO VG46) were used as the working fluids. The corresponding values of the Pr number varied in a wide range 5.5 – 590, and the Re number varied over the range 80 – 50000 depending on the working fluid. It was found that in case of water (Pr $\approx$ 5.5 and Re = 9000 – 50000) the additional insertion of the twisted tape with $y = 5, 10, 15$ into the tube with the enhanced heat-transfer surface did not result in any appreciable augmentation of the heat transfer coefficient, while the noticeable increase of the friction factor was observed. The authors explained such phenomenon as follows. Since a considerable portion of the thermal resistance concentrated in the viscous and buffer sublayers, which was broke by the 3D roughness, the secondary flows, generated due to an additional installation of the twisted tape, did not exert additionally on the convective heat transfer. Such behaviour of the Nu number seems to be a little bit strange, even because the insertion of the twisted tape leads to the increase of the relative effective flow path. Besides, it should be remembered that as the arrangement of the 3D roughness elements remains constant along the surface relative to the tube axis, the additional insertion of the twisted tape results in the change of the attack angle of the mean flow and, correspondingly, it causes the modification of the transversal and longitudinal

pitches of the 3D element relative to the swirl velocity vector. It would be interesting to check such explanation of the observed behaviour by the additional experimental investigation changing only the relevant orientation of the roughness elements on a surface relative to the swirl velocity vector.

In case of applying of ethylene glycol (the Pr number varied over the range 65 – 110) and using the same experimental set-up but covering the flow regimes within the range of the Re number 800 – 6000, Liao & Xin (2000) observed an additional increase of the convective heat transfer for the insertion of the twisted tape, and the increment of the heat transfer was as larger as y was smaller. Furthermore, the difference between values of the St number, corresponding to various y, changed with Re, and it was as larger as Re was smaller.

In case of a turbine oil (ISO VG46, Pr = 320 – 590) for the range of the Re number 200 – 2000, the more considerable increase of the St number was obtained with the additional applying of the twisted-tape insert, that was similar to the experiments with ethylene glycol.

Thus, Liao & Xin (2000) have found that the combination of two enhancement techniques substantially influenced the heat transfer only for the laminar flow regime, whereas this effect was insignificant or missed for the transient and turbulent flow regimes. Moreover, some experiments were performed for the laminar flow with a replacement of the continuous twisted tape by the segmented twisted-tape insert, that led to the more decrease of f as compared with St.

Recently, Zimparov (2002) has considered the combined method of intensification by the spirally corrugated tubes with the twisted tape, that was close to the device offered in the given thesis. The experiments were carried out using water for the flow regimes within the ranges of the Re and Pr numbers $4 \cdot 10^3 - 6 \cdot 10^4$ and $1.9 - 3.7$, respectively, at the constant wall temperature boundary conditions. The additional increase of the heat transfer was observed for the combined use of the single start spirally corrugated tube and the twisted-tape insert. For example, the Nu number of the single start corrugated tube with a pitch of ribbing $H_{360°} = 8.12$ mm, the height of ribs $e = 0.602$ mm, the helix angle $\beta = 82.2°$ and the internal tube diameter $D = 13.65$ mm was 2.5 – 2.6 times greater as compared with the smooth tube at the simultaneous increase of the friction factor of 3.0 – 4.6 times. An additional installation of the twisted tape with the relative twist ratio $y = 3.95$ resulted in the increase of the Nu number 3.5 – 4.4 times at the simultaneous increase of f 7.9 – 10.2 times.

Two years later Zimparov (2004 part1, part2) has made an attempt to develop the simple mathematical model for the prediction of the heat transfer coefficients and friction factors in the fully developed turbulent flow in a spirally corrugated tube combined with the twisted-tape insert. The proposed method was an extension and modification of the idea by Smithberg & Landis (1964) for calculation of the friction factors in the smooth pipes with the twisted tape and took into account the influence of the wall roughness on the axial velocity, the secondary fluid motion, the resulting swirl flow and thermal

resistances of the helicoidal core flow, twisting boundary layer flow as well as the viscous sublayer near the wall.

It is necessary to note the experimental investigation of the thermal-hydraulical characteristics of the combined use of the spirally corrugated tubes and the inlet axial vane swirlers at the condition of cooling of air, which was carried out by Wu *et al.* (2000). The flow regimes varied in range of the Re number $10^4 - 10^5$. The additional increase of the heat transfer of $1.52 - 2.75$ times was also observed at the simultaneous increase of f of $4.21 - 8.49$ times. Moreover, the experimental data for f and Nu were generalized in the form of the dependences of products of f or Nu for the local axial vane swirler and corrugated tube, respectively, in relation to the corresponding values for the smooth pipe, and multiplied by the friction or heat transfer compound coefficient. It was the authors opinion that this coefficient could be determined experimentally and depended on both the Re number and the compound angle, formed between the internal ribbing and the twisted flow behind the vane swirler.

There are also known some compound schemes involving the combining use of the helical corrugated tubes (see, for example, Dzyubenko *et al.* (1994)), that results in the additional increase of the heat transfer.

2. EXPERIMENTAL SETUP

The experimental investigation of the heat transfer was performed directly in the convective part of two fire-tube boilers of a different design. The description of them is presented below. The pressure drop characteristics of the considered heat transfer augmentation techniques were studied for the isothermal conditions by means of the specially designed and constructed experimental set-up. The decision to conduct the experiments on the friction factors in only isothermal condition was taken as a result of the estimation of the possible uncertainties in the pressure drop measurements for the diabatic conditions on the above mentioned fire-tube boilers as well as the analysis of the literature data, concerning the influence of a variability of a gas thermal properties on the convective heat transfer at the cooling conditions. The establishing of the validity of the pressure drop measurements on the fire-tube boilers results in the relatively large uncertainty of the friction factor (more than 60%), that is caused mainly by the buoyancy evaluation, the correction of the variable gas density in the drain tubes and due to that the measured values are relatively small in itself. However, nevertheless, despite the relatively low validity of such measurements, the author of the thesis has made an attempt to perform the measurements in a convective part of the boiler. The results of these measurements were published in the article by Neshumayev *et al.* (2003) (Paper I), and in view of the above mentioned reasons they are not any more discussed in the given thesis. The only one main conclusion of these measurements is that they are in good agreement with the data obtained by the experimental set-up characterized by a high validity.

2.1 Experimental apparatus EA1

The convective flue duct of the fire-tube boiler of the output power about 200 kW consisted of two sequential smoke tube arrays (6, 8 in **Fig. 2**), either of them contained 20 horizontal tubes with the internal diameter $D = 0.051$ m. The first on the flue gas path tube array had the relative length $L/D \approx 21$, and the second one had $L/D \approx 26$. The working fluid was the combustion products of a light oil fuel with the fractional water vapour content of $r_{H_2O} = 0.11 - 0.14$.

During the experiments the temperature of the flue gas at the input/output of the first and second tube arrays (on the flue gas path), the temperature of the cooling water at the input and output as well as the volume flow rate of the cooling water were recorded. The K-type thermocouples with the electrode diameter of 0.5 mm were applied for the flue gas temperature measurements. All the thermocouples were shielded with the threefold nickel foil screens. Additionally, the suction thermocouples were applied at the entrance of the first array, where the higher temperature gas region was located.

At the entrance of the first array three suction thermocouples were positioned along a circle of 90° step increment, at 9, 12 and 15 clock positions, respectively. Similarly, at the entrance of the second part the temperature

measurements were performed using four K-type thermocouples, which were positioned uniformly along a circle of 90° step increment, at 9, 12, 15 and 18 clock positions, respectively.
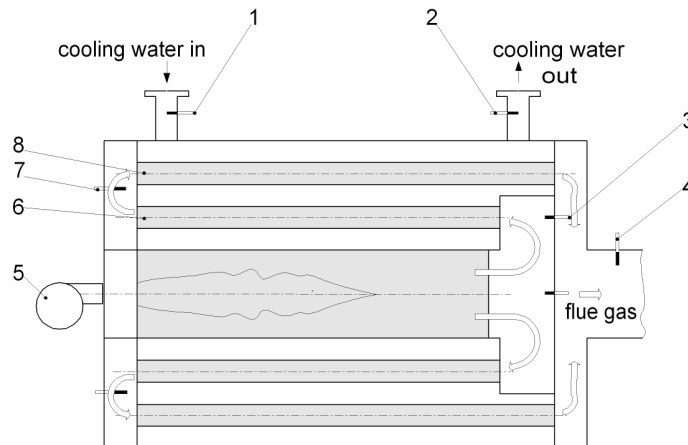
Fig. 2. Schematic of the convective part of the fire tube boiler set-up (the EA1 design): 1,2 – the resistance temperature detector (RTD 100 Ohm); 3 – the suction thermocouple; 4 – the gas analyzer probe, thermocouple; 5 – the light oil burner; 6 – the hot part (HP) zone; 7 – the shielded thermocouple; 8 – the cold part (CP) zone.

The analysis of the combustion products was executed at the end of the flue gas path. In order to determine the radiation heat transfer between the turbulator insert and the internal tube wall, the temperature of surface of some inserts was measured. The K-type thermocouples of the wire diameter of 0.5 or 0.2 mm were used to perform this task. They were placed in three or five locations along a centerline of the turbulator insert.

In accordance with the temperature level at various locations of the convective part of the boiler, the first tube array was conditionally denoted as HP (the hot part, the gas temperature at the entrance was about 1100 °C) and the second one as CP (the cold part, the gas temperature at the entrance did not exceed 500 °C)

The twisted-tape turbulator (**Fig. 3a**) with the relative twist ratio $y = 4.12$ (the 180° twist), the vertical straight tape ($y \to \infty$) with the width equalled to the internal tube diameter and the combined turbulator (**Fig. 3b**), consisting of the internal twisted tape with the twist ratio $y = 2.16$ (at 180° rotational) and the external tape, which was spirally winded on the internal tape, with the longitudinal pitch $h_{360°} = 110$ mm and the relative height of tape (rib) $e/D = 0.098$ (N0a ID-code, see Table 1), were under consideration. The experiments without any inserts were performed for the comparison.
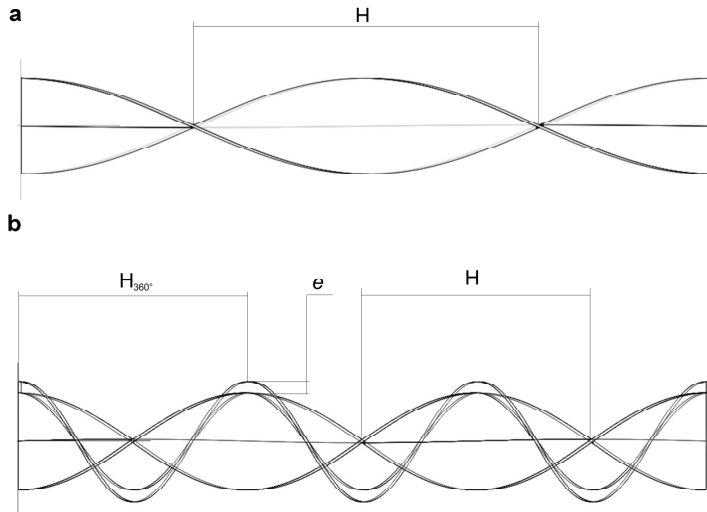
Fig. 3. Schematics of the twisted-tape insert (a) and combined turbulator insert (b).

2.2 Experimental Apparatus EA2

The convective part of the second fire tube boiler of the output power about 20 kW (see **Fig. 4**) consisted of five tubes with the relative length $L/D \approx 18$ and with the internal tube diameter $D = 0.051$ m. The tubes were oriented at a small angle less than $15°$ relative to the vertical axis. The working fluids were the combustion products of a light oil fuel or the wood pellets with the fractional water vapour content of $r_{H_2O} = 0.11 - 0.14$.

The gas temperature at the entrance (one or two sampling points were used) and exit of the convective part, the cooling water temperature at the input and output of the boiler as well as the cooling water volume flow rate were measured. The temperature measurement procedure was
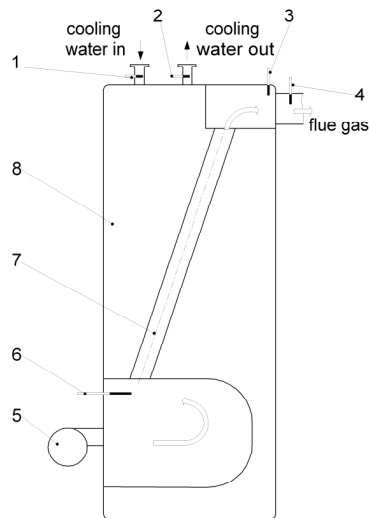
Fig. 4. Schematic of the convective part of the fire tube boiler (the EA2 design): 1,2 – the resistance temperature detector (RTD 100 Ohm); 3 – thermocouple; 4 – the gas analyzer probe, thermocouple; 5 – the light oil or wood pellets burner; 6 – the shielded thermocouple; 7 – the flue gas duct (convective part); 8 – the cooling water-jacket.

29

the same as for the EA1 design case. The analysis of the combustion products was executed at the end of the flue gas path. The given experimental set-up was used for the studying of the mean convective heat transfer characteristics of the combined turbulator inserts N0, N1, N2, N3, N4 as well as the smooth tubes. The geometrical parameters of the inserts are listed in Table 1.

Table 1 The geometrical parameters of the combined inserts

turbulator ID	$H_{180°}$, m	h, m	e, m	δ, m	y	e/D	h/D
N0a	0.11	0.11	0.005	0.0015	2.16	0.098	2.16
N0	0.11	0.11	0.01	0.0015	2.16	0.2	2.16
N1	0.2	0.106	0.0047	0.0015	3.92	0.09	2.08
N2	0.101	0.106	0.0045	0.0015	1.98	0.09	2.08
N3	0.206	0.111	0.009	0.0015	4.04	0.18	2.18
N4	0.122	0.056	0.0037	0.0015	2.39	0.07	1.1

All inserts were made from the metal sheet of thickness $\delta = 1.5$ mm. In the experiments the central heating system of the building was used to provide the steady-state condition of the cooling loop of both boiler design cases (EA1, EA2). The mean cooling water temperature was measured to be from 60 °C to 80 °C. The temperature increase in boilers was recorded to be about 10 – 20 °C. Such a negligible temperature change in both experimental set-ups provide the uniform tube wall temperature boundary condition.

2.3 Experimental Apparatus EA3

The isothermal hydraulic characteristics of inserts N1, N2, N3 and N4 (see Table 1) were studied on the specially designed and constructed experimental set-up EA3 (**Fig. 5**). The given test facility was an U-shaped open contour, where the motion of the working fluid (air of the indoor temperature) was generated by a blower. After leaving the blower the air passed first through the mechanical filter, then through the developing section (~40 calibres), which was followed by the test section of 0.9 m length (about 18 calibres). Further, the air passed through the mass flow measurement section consisting of the PVC tube of 0.018 m diameter with the Honeywell AWM720P1 mass flow sensor, installed in the middle of it.

The developing length and the test section were fabricated from a copper tube of the internal diameter 0.051 m. The internal surface of the tube was carefully polished after the drilling of the static pressure drainage orifices. Eight bores were drilled in a cross-section of each pressure tap. These bores were spaced uniformly along a circle, and they were banked by the ring-type chamber, installed at the external surface of the tube. The pressure taps had the following dimensions: approximately half of the wall thickness, which was counting from the external surface of a tube with the wall thickness about 3.5 mm, had an orifice with a diameter about 0.5 mm, and the rest part of the

wall thickness had the 0.3 mm orifice. The diameters of the pressure taps were chosen according to Repik & Kuzenkov (1989, 1990).
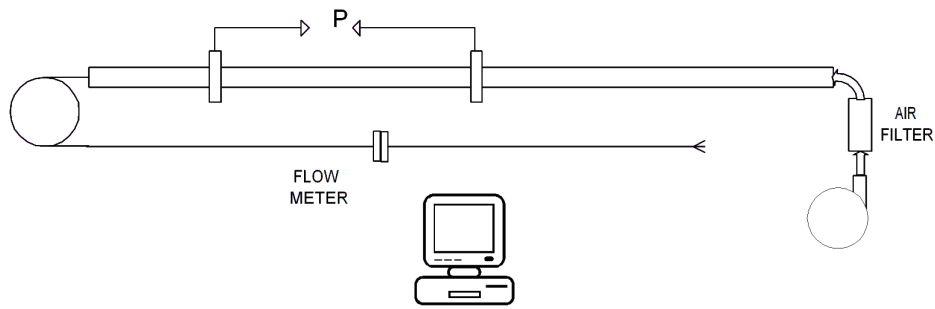
Fig. 5. Experimental apparatus EA3

During the experiments the following parameters were measured: the pressure drop along the test section, the air mass flow and the temperature of the ambient air. The differential pressure transducer of an accuracy about 0.5 % and the measurement limit of 25 Pa, having the built-in amplifier of an output signal from 1 up to 5 Vdc, was used for the pressure drop measurements. The sensor of the mass air flow of an accuracy of the readings less than 7 %, having the built-in amplifier with an output signal from 1 up to 5 Vdc, was applied for the air mass flow measurements. It was impossible to obtain the true data of the friction factor of the smooth tube at the given general hydraulic performance of the test facility for the survey range of the Re number due to the necessity of the measuring of the relatively small pressure drops (less than 1 Pa) and the stabilizing of the flow over a long distance. Therefore, in order to check the validity of the given experimental set-up and the experimental technique, the experiments with the twisted tape of the twist ratio $y \approx 4$ were performed at first.

2.4 Data reduction

The processing of the raw data, obtained for the first two experimental facilities (EA1, EA2), was as follows. The excess air coefficient was calculated from the gas analysis of the combustion products with taking into account the incomplete combustion. The specific (i.e. per the unit mass of a fuel) volume of the combustion products under an atmospheric condition was determined from the known fuel composition and the excess air rate data. The enthalpy of the flue gas was calculated from its specific heat and temperature.

The output power of the boiler was determined from the temperature recordings for the cooling water at the input and output and by the volumetric flow rate. The fuel consumption was determined both from the indirect heat balance and the output power of the boiler. In addition, for a validation of the given calculation method an attempt was made to measure directly the fuel consumption for the EA2 case at the applying of a light oil fuel only. The both

mentioned methods agreed within 3%. The actual volume flow rates of the flue gas and, correspondingly, the average velocities in the tubes were calculated from the fuel consumption data and the fractional composition of the combustion products.

The mean total heat transfer coefficient was determined from the logarithmic-mean temperature difference (the temperature of the wall T_w was calculated) and from the gas enthalpy data, obtained in the convective part of boiler. In case of the smooth pipe (i.e. with no insert) the convective heat transfer coefficient was calculated by taking into account the heat transfer by a radiation due to a high flue gas temperature.

The convective heat transfer coefficient in the presence of turbulator was determined on the basis of the heat flux, which was calculated as the difference between the total mean heat flux (the enthalpy drop along the channel) and the radiation heat flux between the surface of the insert and the internal surface of the tube wall. The calculations of the radiation heat transfer were based on the temperature measurement data obtained from the surface of the insert. In general, the contribution of the radiation heat transfer did not exceed 30 % of the total heat transfer. In addition, for calculations it was taken into account that there was no thermal contact between the internal surface of the tube and the turbulator.

The thermal properties of the flue gas, expressed in the dimensionless numbers, were calculated by the arithmetic average temperature data (the bulk temperature), obtained at the entrance and at the exit of the tube. The internal diameter of the tube was used as the characteristic length for these calculations.

The friction factor (the Darcy friction factor) for the twisted tape or for the combined inserts for the EA3 case was estimated by the following equation:

$$f = \frac{2D^5 \Delta P \pi^2 \rho}{16 L Q_m^2}, \tag{10}$$

where ΔP was the pressure drop measured between the pressure tap sections. It was assumed that the correction for the pressure loss due to the flow acceleration and deceleration at the inlet and outlet of the insert, respectively, was negligible at the discovered range of the Re number. The given assumption was examined through the appropriate calculation and the experimental test.

2.4.1 Variable gas property correction

It was a little more complicate to determine the variable gas property correction factor $(T_b/T_w)^m$ for the given experimental conditions. The experimental investigations by the different researchers indicate that at the gas heating or gas cooling conditions the influence of the variable gas physical properties strongly differs for the smooth pipes. At present there is no generally recognized relation to determine the temperature correction, especially for the gas cooling case.

Most researchers (see, for example, Petukhov (1970)) agree that for the gas cooling case the heat transfer is higher as compared with the case, when the

isothermal conditions are applied. Petukhov (1970) also noted that the experimental dependence of $\mathrm{Nu}_b/\mathrm{Nu}_{0b}$ on $\theta = T_w/T_b$ appeared considerably weak in comparison with the results obtained from the theoretical analysis. At the same time, Petukhov (1970) recommended to use the following relation:

$$\mathrm{Nu}_b/\mathrm{Nu}_{0b} = 1.27 - 0.27\theta, \tag{11}$$

which is valid for $0.5 < \theta < 1$. Under the present experimental conditions, when Eq. (11) is applied, the variable thermal properties of gas could result in the increase of the diabatic Nu_b as compared with the isothermal Nu_{0b}, with a maximum of 19 %.

In the more recent investigation by Kurganov (1992) in gaseous medium, for which the dependences of viscosity μ, the thermal conductivity λ, and the isobaric specific heat c_p can be correlated with the power relations in a wide range of temperatures as follows:

$$\mu/\mu_0 = \left(T/T_0\right)^{n_\mu}; \qquad \lambda/\lambda_0 = \left(T/T_0\right)^{n_\lambda}; \qquad c_p/c_{p0} = \left(T/T_0\right)^{n_c}, \tag{12}$$

where exponents $n_\mu, n_\lambda, n_c > 0$, and the variable properties are also independent on pressure. Kurganov (1992) offered the following expression:

$$\frac{\mathrm{Nu}_b}{\mathrm{Nu}_{0b}} = \left(\frac{\lambda_w}{\lambda_b}\right)^{1/3} \left(\frac{c_{pw}}{c_{pb}}\right)^{1/4} \left(\frac{T_w}{T_b}\right)^{-[0.53+\Phi_1 \lg(\mu_w/\mu_b)]}, \tag{13}$$

where $\Phi_1 = 0.6 + 0.9\tanh[1.894(X - 0.425)]$, $\quad X = 0.01x/D_0$.

Equation (13) at the gas cooling case is valid for $T_w/T_b > 0.5$. The calculations, performed with the applying of Eq. (13) for the present experimental conditions, show the approximate 7 % increase of the ratio $\mathrm{Nu}_b/\mathrm{Nu}_{0b}$.

The analysis of the combined heat transfer in channel performed by Tamonis (1981) has shown that the variable physical properties of gas at the cooling condition had low influence on the heat transfer. In this case, the exponent m in $\left(T_b/T_w\right)^m$ term equals to -0.05. Therefore, the author predicted even a reduction of the diabatic heat transfer as compared with the isothermal heat transfer. For the present experimental conditions the temperature correction factor results in 5 % difference of the heat transfer according to equation by Tamonis (1981).

Ambrazevičius et al. (in Žukauskas (1982)) investigated the heat transfer for the stabilized air flow for the gas temperature up to 2200 °C and for the nitrogen flow for the gas temperature up to 3730 °C as well in tubes with the wall temperature of 77 °C. The authors have shown that the generalization of the experimental data by the dimensionless heat transfer numbers, using the fluid bulk temperature T_b in the given cross-section and the internal diameter as the characteristic length, should not include an additional simplex of temperatures $\theta = T_w/T_b$ in the well-known heat transfer equation. The general review performed by the same author (Ambrazevičius (2003)) of the main experimental

and theoretical investigations, performed during XX century, has confirmed this statement.

The maximum value of the exponent *m* provided in the literature, seemingly is 0.45 (Gnielinski (1976)). It is possible that in some experiments under the correction factor of the variable thermal gas property other phenomena exist. In these experiments such correction factors just describe the specific experimental condition, for which they were obtained.

At the heating or even the cooling flow condition, using various turbulators and/or inserts (the twisted tape), the influence of the non-isothermal gas flow is yet poor examined. For example, Lopina & Bergles (1969) applied the twiddle factor D_h/D to the value of the correction factor of the variable properties for a twisted flow at the heating condition, that took into account the thermal boundary layers on the internal surface of tubes and on the twisted tape, which are not the same.

Vilemas *et al.* (1989)[5] have performed the experimental investigation of influence of the variable physical gas properties on the convective heat transfer in the annular channels with an artificial roughness for the heating conditions. It was found that influence of the variable physical properties on the heat transfer in the rough channels changed depending on Re. The influence of Re on *m* was more significant for the bigger relative height of the roughness elements. At smaller Re this influence was stronger for the rough channels than for the smooth ones, and at large Re it was weaker. As the temperature factor ratio increased, the transition from the transient mode of roughness to full one shifted towards the larger Re.

Thus, all aforesaid allows to draw the conclusion that at the heating condition the influence of the variable physical properties on the convective heat transfer in the rough channels differs from the one, that occurs for the smooth channel. Nevertheless, due to absence of the true data for the cooling condition in the rough channels and/or for the twisted tape, the temperature correction factor is assumed to be equal unity in the data processing like in case of the smooth pipe insert, i.e. $\left(T_b/T_w\right)^m = 1$.

2.5 Experimental uncertainty

The single-sample uncertainty analysis with the 95 % confidence level using the direct computer-executed method by Moffat (1988) shows the uncertainties of 20 – 40 % for the Nusselt number, and 15 – 35 % for the Reynolds number. Here, the smaller numbers relate to the EA1 case and the bigger ones concern the EA2 case.

The uncertainty of the friction factor for the EA3 test facility was estimated in accordance with Moffat (1988) within the 95 % confidence level as follows:

---

[5] Here the data are cited only for the stabilized flow; authors have obtained data for the inlet section as well.

$$\delta f = \left\{ \sum_{i=1}^{N} \left(\frac{\partial f}{\partial X_i} \delta X_i \right)^2 \right\}^{1/2} \quad , \tag{14}$$

where X_i are the independent variables incorporated in Eq. (10).

The uncertainties of f for the twisted tape were about $16 - 25\,\%\%$ and for combined insert were roughly $15\,\%$. Here, the larger numbers relate to the smaller values of Re.

3. NUMERICAL CALCULATION

3.1 Problem Statement

The present numerical study deals with the combined insert having the following geometrics: $H_{180°} = 0.1$ m, $h_{360°} = 0.1$ m, $e = 0.005$ m. In order to represent the conditions, which are similar to the EA1 case of the experimental program for the N0a insert (see Table 1) and, correspondingly, to enable the comparison with the experimental data, the 3D case and the horizontal orientation are under consideration.

Since the geometrics of the considered combined insert have a periodicity in the longitudinal direction (the pitch of the internal and external helix tapes is constant), the computational domain is selected as the section of the tube, where the external helix tape makes one full turn and the internal twisted tape makes one half of a turn, thus forming the periodicity of geometry with a shift equalled 0.1 m. The given computational domain is presented in **Fig. 6** (see also **Fig. 3b**, where the considered turbulator is shown). Thus, it is assumed that the flow characteristics have a certain longitudinal periodicity (the more precise description of periodicity of the flow parameters will be presented below), and the flow can be considered as the fully developed periodic one.
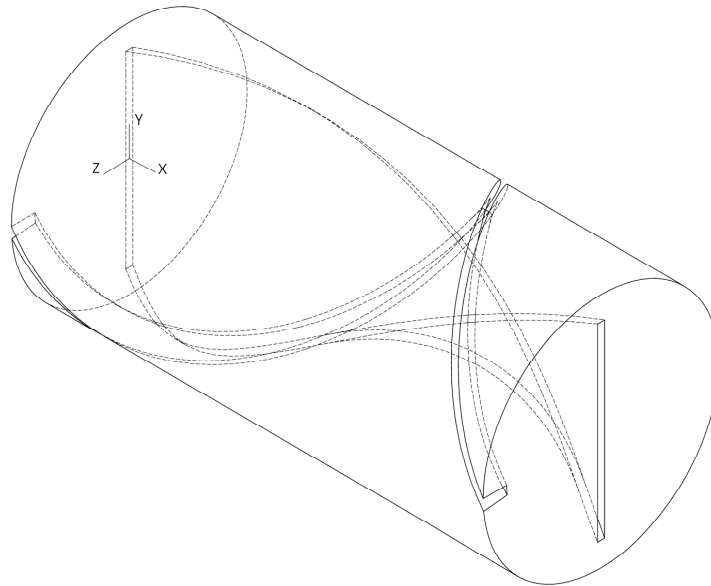
 Fig. 6. Computational domain

The calculations were performed both under the adiabatic conditions and for a presence of the convective heat transfer near the internal surface of a tube (in this case the insert is treated as the adiabatic too). The preliminary calculations have also shown that the buoyancy forces arising from the density variation for the horizontal orientation of a tube are negligible as compared with the inertial

forces and, therefore, the influence of the free convection can be disregarded at the given stage.

All the computations considered air as the working fluid ($Pr \approx 0.7$). The required initial data were chosen based on the condition of compliance of range of the flow Re number to ones occurred in the experimental part of the given investigation. The initial data and also some thermalhydraulic characteristics of the survey flow are presented in Tables 2 and 3. Here the internal diameter of a tube was used for the calculation of the dimensionless numbers.

Table 2 The initial data for the adiabatic conditions (the fluid density is 1.225 (kg/m³), the fluid viscosity is 1.78940E-05 kg/(m s))

Calculation ID	mass flow, kg/s	fluid velocity, m/s	Re
ad1	0.0007	0.30	1034
ad2	0.001	0.43	1476
ad3	0.0015	0.65	2215
ad4	0.002	0.86	2953
ad5	0.0025	1.08	3691
ad6	0.003	1.29	4429
ad7	0.0035	1.51	5168
ad8	0.004	1.73	5906

Table 3 The flow characteristics for the diabatic conditions ($T_{wall} = const \approx 333$ K)

Calculation ID	mass flow, kg/s	$T_{upstream}/T_{bulk,inlet}$ *, K	mean fluid velocity, m/s	Re
d1_300	0.0012	573.15/554.9	0.96	1125
d2_300	0.0026	573.15/553.8	2.13	2408
d3_300	0.0044	573.15/564.9	3.81	3937
d4_300	0.0061	573.15/563.9	5.31	5440
d1_400	0.0014	673.15/646.1	1.31	1190
d2_400	0.0029	673.15/645.4	2.79	2422
d3_400	0.0048	673.15/656.3	4.99	3798
d4_400	0.0068	673.15/649.3	7.25	5280
d1_600	0.0024	873.15/816.8	2.61	1844
d2_600	0.0048	873.15/813.5	5.62	3509
d3_600	0.0072	873.15/826.8	8.71	5133
d4_600	0.0095	873.15/832.0	11.66	6685

* - the first value is the bulk temperature of the flow specified on the inlet; the second value is the upstream bulk temperature obtained by the calculation, which explanation is adduced below in Eq. 33.

In order to estimate the accuracy of the numerical simulation (in terms of the integral values only), the numerical results were compared with the experimental data obtained in the experimental part of the present research.

3.2 Mathematical formulation and turbulence models

The given numerical study deals with the steady-state incompressible fluid without taking into account the possible influence of the gravitational forces.

The Reynolds-averaged Navier-Stokes (RANS) equations written for the Cartesian coordinate system with applying of the tensorial form are as follows (Fluent 6.1 User's guide, Versteeg and Malalasekera (1995)):

(the continuity equation)

$$\frac{\partial}{\partial x_i}\left(\rho\, U_i\right) = 0, \tag{15}$$

(the momentum equation)

$$\frac{\partial}{\partial x_j}\left(\rho\, U_i U_j\right) = -\frac{\partial P}{\partial x_i} + \frac{\partial}{\partial x_j}\left[\mu\left(\frac{\partial U_i}{\partial x_j} + \frac{\partial U_j}{\partial x_i}\right)\right] + \frac{\partial}{\partial x_j}\left(-\rho\overline{u_i' u_j'}\right). \tag{16}$$

In the latter equation the Reynolds stresses were modelled considering the Boussinesq hypothesis:

$$-\rho\overline{u_i' u_j'} = \mu_t\left(\frac{\partial U_i}{\partial x_j} + \frac{\partial U_j}{\partial x_i}\right) - \frac{2}{3}\rho k\delta_{ij}. \tag{17}$$

RNG k-ε turbulence model

The Renormalization Group (RNG) $\kappa-\varepsilon$ turbulence model (see, for example, Choudhury (1993)) was used for the closure of the above-stated equations. The given turbulence model was elaborated on the basis of the instantaneous equations of the momentum conservation by the applying of the mathematical statistics methods, called as the Renormalization Group (RNG). The essence of this model is that the small-scale eddies terms are removed from the Navier-Stokes equations by means of the RNG methods with applying of the iterative approach and the expressing of the small-scale eddies effects in term of the larger scale motions and the modified viscosity.

This model was chosen as the basic for the realization of the numerical simulation for the given study. The main arguments advanced in favour of the chosen turbulence model as compared with the conventional k-ε model as well as the problem, which is considered in the given study, were the following:

- the constants and functions included in the given model are obtained on the basis of theory and, thus, there is no necessity of their adaptation to the conditions of the given research;
- the new term is introduced into the dissipation rate transport equation (R_ε, see Eq. (19)), that enables to improve the accuracy of the calculations of the highly strained flows (the twisted flows etc.)
- the RNG theory also results in the theoretical dependences for some modelled variables at small Re numbers (for example, for μ_t).

38

The transport equations for the RNG k-ε model are as follows:

$$\frac{\partial}{\partial x_i}\left(\rho k\, U_i\right) = \frac{\partial}{\partial x_j}\left(\alpha_k \mu_{eff}\frac{\partial k}{\partial x_j}\right) + G_k - \rho\varepsilon, \tag{18}$$

$$\frac{\partial}{\partial x_i}\left(\rho\varepsilon\, U_i\right) = \frac{\partial}{\partial x_j}\left(\alpha_\varepsilon \mu_{eff}\frac{\partial\varepsilon}{\partial x_j}\right) + C_{1\varepsilon}\frac{\varepsilon}{k}\left(G_k\right) - C_{2\varepsilon}\rho\frac{\varepsilon^2}{k} - R_\varepsilon, \tag{19}$$

where μ_{eff} is the effective viscosity, $\mu_{eff} = \mu + \mu_t$.

The differential equation for the turbulent viscosity under the RNG theory:

$$d\left(\frac{\rho^2 k}{\sqrt{\varepsilon\mu}}\right) = 1.72\frac{\hat{v}}{\sqrt{\hat{v}^3 - 1 + C_v}}d\hat{v}, \tag{20}$$

where $\hat{v} = \mu_{eff}/\mu$, $C_v = 100$.

In the above-mentioned equations the inverse effective Prandtl numbers, namely α_k and α_ε, were computed using the following formula:

$$\left|\frac{\alpha - 1.3929}{\alpha_0 - 1.3929}\right|^{0.6321}\left|\frac{\alpha + 2.3929}{\alpha_0 + 2.3929}\right|^{0.3679} = \frac{\mu}{\mu_{eff}}, \tag{21}$$

where $\alpha_0 = 1.0$.

The production of the turbulence kinetic energy term included in Eq. (18) is as follows:

$$G_k = -\rho\overline{u_i' u_j'}\frac{\partial U_j}{\partial x_i}. \tag{22}$$

The R_ε term in the ε equation (Eq. (19)) is as follows:

$$R_\varepsilon = \frac{C_\mu \rho\eta^3\left(1 - \eta/\eta_0\right)}{1 + \beta\eta^3}\frac{\varepsilon^2}{k}, \tag{23}$$

where $\eta \equiv Sk/\varepsilon$, $\eta_0 = 4.38$, $\beta = 0.012$. S is the modulus of the mean rate of the strain tensor, $S \equiv \sqrt{2S_{ij}S_{ij}}$.

The model constants $C_{1\varepsilon} = 1.42$ and $C_{2\varepsilon} = 1.68$.

Low Reynolds k-ε turbulent model
Some calculations were performed also with the application of the well-known modified κ–ε turbulence model, elaborated for small Reynolds numbers (see, for example, Versteeg & Malalasekera (1995)), where the damping functions were introduced into the transport equations of the kinetic energy, the dissipation rate equation as well as the equation for the turbulent viscosity.

In the given research the Lam and Bremhorst wall-damping functions were used only. These functions look like:

$$f_\mu = \left[1 - \exp\left(-0.0165\,\mathrm{Re}_y\right)\right]^2 \left(1 + \frac{20.5}{\mathrm{Re}_t}\right); \tag{24}$$

$$f_1 = \left(1 + \frac{0.05}{f_\mu}\right)^3 ; \tag{25}$$

$$f_2 = 1 - \exp\left(-\mathrm{Re}_t^2\right), \tag{26}$$

where $\mathrm{Re}_t = \dfrac{\rho k^2}{\mu \varepsilon}$, $\mathrm{Re}_y = \dfrac{\rho \sqrt{k}\, y}{\mu}$, $\mathrm{Re}_\varepsilon = \dfrac{\rho (\mu \varepsilon / \rho)^{1/4}\, y}{\mu}$.

Turbulent heat transfer
The turbulent heat transfer is described within the given study by the following equation:

$$\frac{\partial}{\partial x_j}\left(\rho\, \mathrm{U}_j \mathrm{T}\right) = \frac{\partial}{\partial x_j}\left(k_{eff}\, \frac{\partial T}{\partial x_j}\right), \tag{27}$$

where $k_{eff} = \alpha c_p \mu_{eff}$ is the effective thermal conductivity, and α is calculated by Eq. (21) with $\alpha_0 = k / \mu c_p$.

3.3 Periodic and boundary conditions
The periodicity condition of the fully developed flow is assumed within the present study. This condition was introduced by Patankar *et al.* (1977), and it allows to obtain the solution of the problem without a solving of the stabilization section of the tube. The periodicity conditions for the velocity components, the pressure drop and temperature of the fluid are expressed as follows:

$$u_i(\vec{r}) = u_i(\vec{r} + \vec{L}) = u_i(\vec{r} + 2\vec{L}) = ..., \tag{28}$$

$$\Delta p = p(\vec{r}) - p(\vec{r} + \vec{L}) = p(\vec{r} + \vec{L}) - p(\vec{r} + 2\vec{L}) = ..., \tag{29}$$

$$\theta(\vec{r}) = \theta(\vec{r} + \vec{L}) = \theta(\vec{r} + 2\vec{L}) = ..., \tag{30}$$

where $\vec{r}$ is the position vector, and $\vec{L}$ is the periodic length vector.
   The pressure gradient can be also decomposed into two parts:

$$\nabla p(\vec{r}) = \beta \frac{\vec{L}}{\left|\vec{L}\right|} + \nabla \tilde{p}(\vec{r}), \tag{31}$$

where $\beta = p(\vec{r}) - p(\vec{r} + \vec{L})$, and the second term of the second member of the given equation expresses the local fluid motion and it is periodic.

In Eq. (30) θ is the dimensionless periodic fluid temperature, and for the constant wall temperature boundary condition it is defined as:

$$\theta = \frac{T(\vec{r}) - T_{wall}}{T_{bulk,inlet} - T_{wall}}, \qquad (32)$$

where $T_{bulk,inlet}$ is the bulk temperature at the inlet:

$$T_{bulk,inlet} = \frac{\int_A T \left| \rho \vec{v} \cdot d\vec{A} \right|}{\int_A \left| \rho \vec{v} \cdot d\vec{A} \right|}, \qquad (33)$$

where A is the inlet periodic boundary.

The following boundary conditions were applied for the given calculations. The constant temperature of the wall was set on the internal surface of the tube (see Table 3). The adiabatic conditions were set on the surfaces of the internal and external helical tapes. The no-slip boundary condition was implemented on the walls.

3.4 Numerical Solution Procedure

The numerical solution of the differential equations for the above-mentioned mathematical statement was performed with the help of the available commercial CFD code FLUENT 6.1.22, and the geometry and the grid of the computational domain were prepared by the GAMBIT 2.1.6 software.

The computational domain shown in **Fig. 6** was discretized by the non-unisize (normal to the wall) unstructured 3D tetrahedral meshes. The finest grid was located on/near the walls of the tube and insert as well. Besides, the mesh size on the surface of the external tape of the combined insert and in its vicinity was additionally reduced (**Fig. 7**).

Table 4 shows the sizes of the applied mesh elements expressed in the absolute and dimensionless units, normalized by the dynamic velocity $U_\tau = \sqrt{\tau_w / \rho}$ and the kinematic viscosity. The shear stress included in this equation was computed as the area-weighted integral for the appropriate surface by the numerical simulation. Since in the given study the absolute size of the mesh elements at various calculations remained invariable, the dimensionless size, expressed in terms of y^+, increased. The retention of constancy the dimension of the mesh elements in terms of the wall units y^+ was not applied because of the limitation of the power resources of the available computer.

Table 4 Some characteristics of the applied computational grid

ID	surface	mm	y^+	ID	surface	mm	y^+
	rib	0.4	1.915		rib	0.4	4.76
ad1	tape	0.7	3.593	d3_300	tape	0.7	10.12
	tube	0.7	2.484		tube	0.7	6.76
	rib	0.4	2.519		rib	0.4	6.27
ad2	tape	0.7	4.597	d4_300	tape	0.7	12.02
	tube	0.7	3.413		tube	0.7	8.93

41

ad3	rib	0.4	3.128	d1_400	rib	0.4	2.76
	tape	0.7	6.203		tape	0.7	4.35
	tube	0.7	4.535		tube	0.7	3.47
ad4	rib	0.4	4.279	d2_400	rib	0.4	3.34
	tape	0.7	7.768		tape	0.7	6.73
	tube	0.7	6.114		tube	0.7	4.86
ad5	rib	0.4	4.821	d3_400	rib	0.4	6.27
	tape	0.7	9.186		tape	0.7	10.71
	tube	0.7	7.132		tube	0.7	8.39
ad6	rib	0.4	5.851	d4_400	rib	0.4	6.66
	tape	0.7	10.404		tape	0.7	11.79
	tube	0.7	8.229		tube	0.7	9.98
ad7	rib	0.4	6.241	d1_600	rib	0.4	2.61
	tape	0.7	12.414		tape	0.7	5.54
	tube	0.7	9.007		tube	0.7	3.79
ad8	rib	0.4	6.888	d2_600	rib	0.4	4.14
	tape	0.7	12.499		tape	0.7	8.37
	tube	0.7	10.511		tube	0.7	5.91
d1_300	rib	0.4	2.29	d3_600	rib	0.4	5.53
	tape	0.7	4.12		tape	0.7	11.16
	tube	0.7	2.93		tube	0.7	8.02
d2_300	rib	0.4	3.61	d4_600	rib	0.4	7.23
	tape	0.7	6.53		tape	0.7	13.34
	tube	0.7	4.92		tube	0.7	10.70

In calculations for the adiabatic conditions and small Re numbers (ad1 and ad2 cases), the attempt was made to additionally refine the grid in order to estimate the influence of the mesh size on the final result in the regions, where the velocity gradient was the largest. The given refinement did not result in any significant difference of the final results, therefore, and also due to the low computing resources, no additional refining of the grid was applied.

The linearization and the subsequent solving of the discretized equations were performed with the applying of the segregated solution method due to the imposed limitation when using the periodic boundary conditions. The second-order upwind scheme was applied in all the calculations to obtain the cell faces values of the control volume (since the FLUENT code used a co-located scheme), including the governing equations of impulse, turbulent kinetic energy, the energy dissipation rate and energy. The Node-Base scheme was applied for the derivative evaluation. The PRESTO! scheme was used for the pressure interpolation. The SIMPLE algorithm was used for the coupling between pressure and velocity.
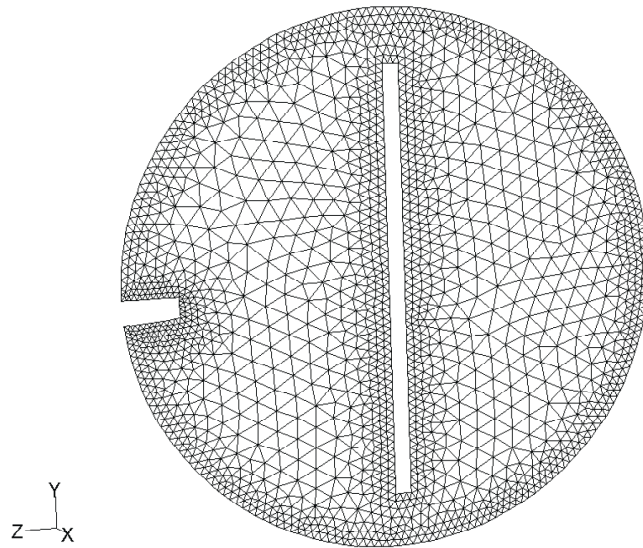
Fig. 7. Example of grid for the computational domain at the inlet cross-section

4. RESULTS AND DISCUSSION

4.1 Thermalhydraulic characteristics of the smooth tubes and tubes with the straight and twisted-tape inserts

Heat transfer (total and convective) characteristics

In order to verify the applied experimental techniques and the measuring circuit, the experiments with the smooth tubes (having no inserts), tubes with the straight tape ($y \to \infty$, the vertical orientation in tubes) and tubes with the twisted-tape insert ($y = 4.12$) were performed.

Fig. 8 shows the experimental data of the heat transfer in the smooth horizontal tubes obtained in the EA1 case for two various convective parts (HP and CP). The solid data points (circles, squares, and triangles) presented on this chart were obtained from the calculations, which were performed by three different methods as follows. The first two calculation methods presented below were based on the assumption of the distribution law of the bulk gas temperature along the channel and on the subsequent computation of the local heat transfer coefficients. The gas temperature distribution function was assumed to be exponential along the channel because of the uniform wall temperature boundary condition. Therefore, the mean heat transfer coefficient was determined according to Isachenko *et al.* (1981) as follows:

$$\alpha_m = \frac{\displaystyle\int_0^L (\alpha \Delta t)\, dx}{\displaystyle\int_0^L \Delta t\, dx}. \tag{34}$$

The first calculation method (denoted by the solid circles in **Fig. 8**) was performed using the equations by Tamonis (1981) under the assumption that the turbulent boundary layer developed at the edge of the tube and the boundary of the transition to the stabilized flow was determined by the approximate equation by Kutateladze (1990):

$$x_0 \ge 0.6 D\, \mathrm{Re}^{0.25}. \tag{35}$$

According to Tamonis (1981), in calculations the dimensionless turbulence scale K_t and the turbulent Prandtl number Pr_t at the cooling conditions of the combustion products were assumed to be $K_t = 0.14$ and $Pr_t = 0.2$ for the fully developed turbulent flow.

In the second calculation method, the local heat transfer coefficient was calculated by the Petukhov-Kirilov equation (the results are denoted by the solid square boxes in **Fig. 8**):

$$Nu = \frac{\left(f_{darcy}/8\right) \mathrm{Re}\, \mathrm{Pr}\, c_t}{1 + 900/\mathrm{Re} + 4.5\sqrt{f_{darcy}}\left(\mathrm{Pr}^{2/3} - 1\right)}, \tag{36}$$

where the Darcy friction factor f was determined as $f_{darcy} = (1.82 \lg \mathrm{Re} - 1.64)^{-2}$.

The correction factor of the thermal entrance effect c_t was determined according to Žukauskas (1982) on the assumption that the turbulent boundary layer developed at the edge of the tube and, correspondingly, the stabilization of the heat transfer coefficient occured in the same manner as in the presence of the calming length:

$$c_t = 1 + 0.48(D/x)^{0.25}\left(1 + 3600/\left(\mathrm{Re}\sqrt{x/D}\right)\right)\exp(-0.17\,x/D). \qquad (37)$$

The third calculation method of the mean heat transfer coefficient was performed with taking into account the relative length of the channel and applying the well-known Gnielinski's equation (Gnielinski, (1976)):

$$\mathrm{Nu}_m = \frac{\left(f_{darcy}/8\right)\left(\mathrm{Re} - 1000\right)\mathrm{Pr}}{1 + 12.7\sqrt{f_{darcy}/8}\left(\mathrm{Pr}^{2/3} - 1\right)} \cdot \left[1 + \left(\frac{L}{D}\right)^{-2/3}\right]. \qquad (38)$$

The results of those calculations are denoted by the solid triangles in **Fig. 8.**
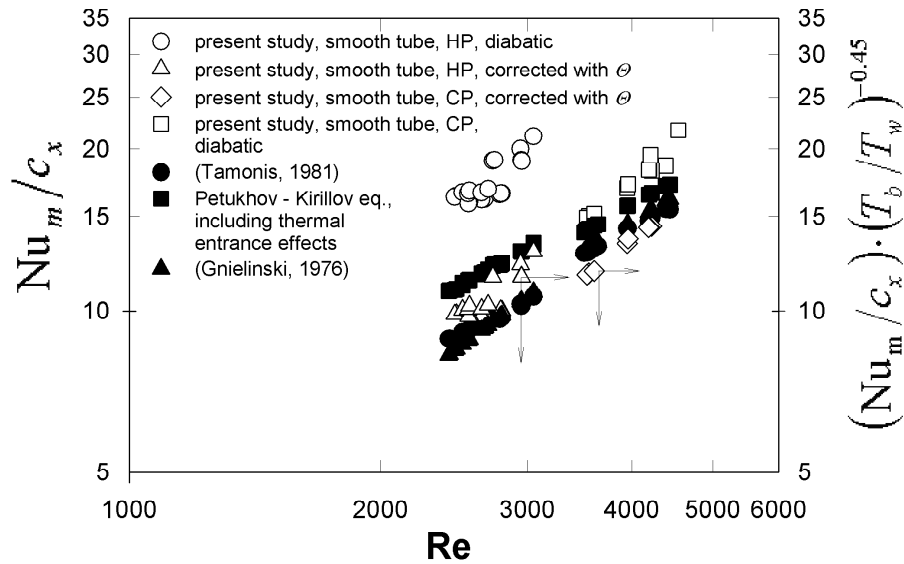
Fig. 8. The results of the heat transfer in the smooth horizontal tube (without a turbulator) in the EA1 design case

One can see from **Fig. 8** that the experimental convective heat transfer coefficient in the hot part (HP) is much higher than the one obtained from the calculations, whereas this difference for the cold part (CP) is not so high and it remains within the limits of accuracy. Obviously, the entrance effects occurred at the entrance of the gas flow at the right angles cause large variations of the level of the heat transfer. However, it should be noted that if one imposes the temperature correction factor with the exponent value of $m = 0.45$ on the experimental data (the right axis of ordinates in **Fig. 8**), which is seemingly the

45

maximum value of the exponent *m* provided by the literature (see, for example, Gnielinski (1976)), it is possible to achieve a satisfactory agreement with the calculation results for the isothermal conditions. It just shows that the existing entrance effects, that are responsible for the heat transfer increase, can be described by the introduction of the temperature correction factor.

The experimental results of the heat transfer obtained in the EA2 case for the smooth tubes, having small incline relative to the vertical axis (<15°), are shown in **Fig. 9** versus Re. Here, as it was shown by Bohne & Obermeier (1986), the small inclination of tubes from the vertical axis does not have a strong influence on the heat transfer and, therefore, further it is assumed that the behaviour of the heat transfer is identical for the vertical tubes. Unfortunately, due to the technical restrictions of the EA2 experimental set-up, the experimental data obtained in this research are within a narrow range of the Re numbers, that covers only the laminar flow regime.

It is known that for the case of the mixed convection conditions, when the direction of the buoyancy force is opposite to the forced flow (in our case at the cooling the hot fluid is directed from below upward) occurred in the laminar flow case, the heat transfer decreases as compared with the laminar flow without the buoyancy force present. However, it is also known that the transition of the mixed laminar flow to the mixed turbulent flow in the vertical pipes occurs at the smaller values of Re as compared with the flow case, when the stability loss occurs in the isothermal laminar flow (see, for example, Petukhov & Polyakov (1986)). According to Spalding & Taborek (1983) and on the basis of the similarity parameters Re and Ra_{LM} observed in the current research, the flow regime is taken to be transient. Thus, on the basis of the above-stated, the correlations of the mixed turbulent convection flow are applied for the comparison with the experimental data of the present research (the EA2 design), which were obtained in the smooth tube.

The heat transfer coefficient for the mixed convection was determined according to Aicher & Martin (1997) as the result of the superposition of the pure natural and the pure forced convections as follows:

$$\mathrm{Nu}_{M,O} = \sqrt{Nu_F^2 + Nu_N^2} \ . \tag{39}$$

Here, the heat transfer coefficient for the pure forced convection flow was calculated by the formula for the laminar flow by Aicher & Martin (1997):

$$\mathrm{Nu}_F = \left[3.66^3 + 0.7^3 + \left[1.615 \sqrt[3]{\mathrm{Gz}} - 0.7 \right]^3 + \left[\left(\frac{2}{1+22\mathrm{Pr}} \right)^{1/6} \sqrt{\mathrm{Gz}} \right]^3 \right]^{1/3} . \tag{40}$$

The heat transfer coefficient for the pure natural convection was calculated by Churchill's equation from Spalding & Taborek (1983) as follows:

$$\mathrm{Nu}_N = \frac{(1/128)\mathrm{Ra}^*}{\left\{ 1 + \left(4/(128 \cdot 3) \right)^{3/2} \left[1 + \left(0.492/\mathrm{Pr} \right)^{9/16} \right]^{2/3} \left(\mathrm{Ra}^* \right)^{9/8} \right\}^{2/3}} , \tag{41}$$

where Ra^* is the modified Rayleigh number:

$$\mathrm{Ra}^* = \frac{g\rho^2 c_p \beta (T_b - T_w) D^4}{L\lambda\mu} \qquad (42)$$

Fig. 9 shows that the obtained experimental heat transfer is larger than the heat transfer obtained according to Eq. (39). Most likely, as for a case of a horizontal tube, this can be attributed, for the most part, to the presence of strong entrance effects, which are initiated at the entrance of the gas flow at the right angles. It should be noted that the introduction of the temperature correction factor with the exponent $m = 0.45$ into the experimental data results in a satisfactory agreement with the results obtained by Eq. (39). This is identical to the heat transfer behaviour observed in the horizontal tubes of the EA1 design case.
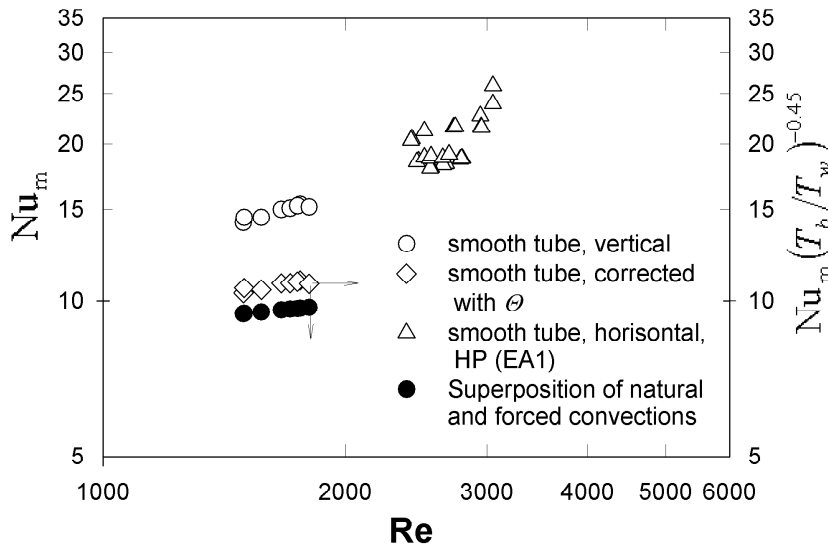
Fig. 9. The results of the heat transfer in the smooth vertical tubes in the EA2 design case.

In spite of the fact that the convective part of the considered experimental facilities consisting of the relatively short tubes, where under the given thermalhydraulic conditions the process of the heat transfer was determined by the set of various factors, that are hardly taken into account, the obtained results can be considered only as the qualitative validation of the applied experimental technique. Under these circumstances, the more rigorous method of verification of the experimental technique will be the additional installation of the twisted tape. The results on the heat transfer both for the twisted tape and the straight tape will be presented below.

Fig. 10 shows the total heat transfer coefficient, which was determined by the enthalpy difference along the tubes, and the convective (from the gas flow to the internal surface of the tube) heat transfer coefficient for the twisted and

47

straight tapes in the horizontal channels obtained for the EA1 design case. In spite of the fact that the experimental data obtained for the straight tape have a little larger scattering, some qualitative conclusions can be drawn.

The temperature measurements at the surface of the inserts have shown that the mean integral temperature of the surface in HP of the twisted-tape insert was greater as compared with the straight tape insert. Probably, it means that the convective heat transfer from the gas flow to the surface of the twisted-tape turbulator is higher in comparison with the value obtained for the flat tape insert. This follows from the identity of the emissivity characteristics of both types of inserts and equality of the convective and radiation heat fluxes, i.e. such that $q_{TURB}^{C} = q_{TURB}^{R}$. However, the opposite situation is observed in the cold part, indicating that the convective heat transfer to the surface of the straight tape is higher.

As follows from **Fig. 10**, the radiation heat transfer for the twisted tape insert remains at the same level for both HP and CP zones, while for the flat tape it is higher in the CP zone. Such behaviour may be partially attributed to the existing strong entrance effects, which could be suppressed by the twisted tape and could only take place for the flat tape case.
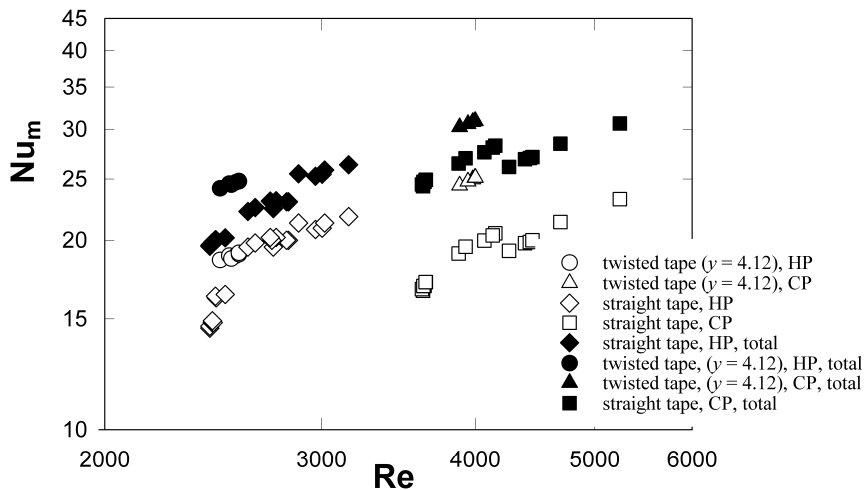
Fig. 10. The results of the total and convective heat transfer in the EA1 design case.

Generally, the total heat transfer coefficient for the twisted tape is larger than for the straight tape. The convective heat transfer coefficients for both types of inserts are approximately the same in the HP zone, while in the CP zone the convective heat transfer coefficient for the twisted tape is noticeably greater than for the straight tape case. It should be also noted that the experimental results obtained for the smooth tube, which are not presented in **Fig. 10**, are quite similar to the convective data obtained for the flat tape insert.

48

The results of the convective heat transfer of the twisted and the straight tape inserts, obtained for the EA1 design case are presented in **Fig. 11**. In addition, the generalized correlation for the laminar-transition turbulent flow for the twisted tape, derived by Manglik & Bergles (1993a, b) for three values of y in the absence of the free convection due to $Gr < Sw^2$, are also presented in **Fig. 11**. As one can see from **Fig. 11**, the experimental results for both CP and HP zones for the twisted-tape insert lie below the ones calculated by Eq. (9). This difference is about 17% in the HP zone, while in the CP zone it is smaller for the same twist ratio $y = 4.12$. This could be partially attributed to the fact that at the cooling conditions the centrifugal convection in the twisted flow results in the displacement of the more cold volumes of the fluid to a peripheral area of the tube, and this may become the undesirable factor, which is even capable of the reduction of the heat transfer. The agreement with the correlation (Eq. (9)) within 17 % difference can be also the validation of the given experimental set-up. In addition, the characteristic trend of the experimental data of the twisted tape shown in **Fig. 11** indicates that the heat transfer coefficient does not depend on the relative length of the tube L/D for the considered range of L/D.
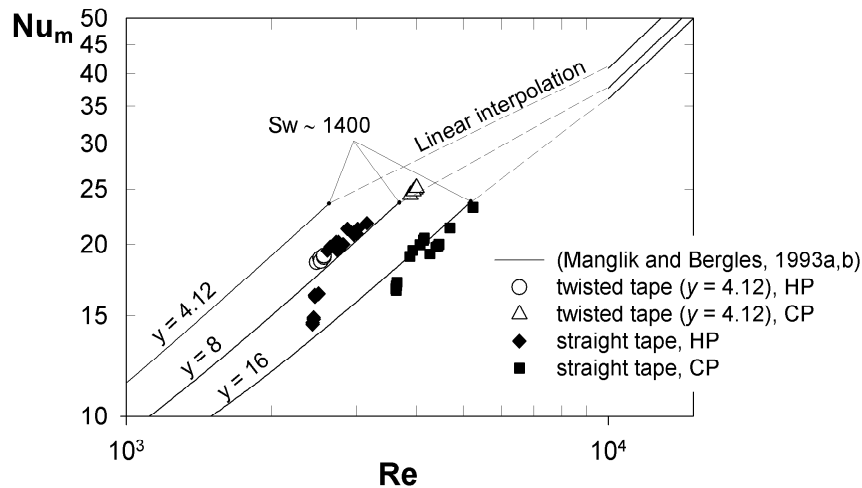
Fig. 11. The results of the convective heat transfer for the twisted and straight tapes (the EA1 design case).

Pressure drop characteristics
The experimental research of the hydraulic characteristics of the combined inserts was performed by the EA3 test facility only for the isothermal conditions by the reasons that were stated above. The preliminary validation tests of the used experimental procedure were carried out using the twisted tape of $y = 4.12$,

whereas the appropriate data for the smooth tube were not taken into account, as it was impossible to obtain the reliable data for the given flow regime (Re = 1000 – 5000) and for the given design of the test facility (the relatively short flow developing section etc.).

Figs. 12 and **13** show the experimental dependences of the friction factor for the twisted tape on the De and Re numbers, respectively. Here, the hydraulic diameter was used as the characteristic length for the calculation of the friction factor in the first case. The experimental data by Budov & Dmitriev (1989) and Manglik & Bergles (1993 a, b) are presented in these figures for comparison, respectively. Budov & Dmitriev (1989) proposed the following relation for the laminar flow regime accompanied with the macro eddies which has accuracy less than 9%:

$$f(Darcy)_{Dh} = \frac{6.34}{\mathrm{Re}_h^{0.474}} \left(\frac{D_h}{D_{hel}} \right)^{0.263} + \frac{25.6}{\mathrm{Re}_h}, \qquad (43)$$

where D_{hel} is a diameter of curvature of a centre line of the channel formed by the tube and the twisted tape.

The uncertainties within the 95 % confidence level of the given experiment are also shown (the dash line, **Fig. 13**). As follows from **Figs. 12** and **13**, there is a good agreement of the presented experimental data with the relations available from the literature, that is the evidence of the validity of the applied experimental technique and procedure.
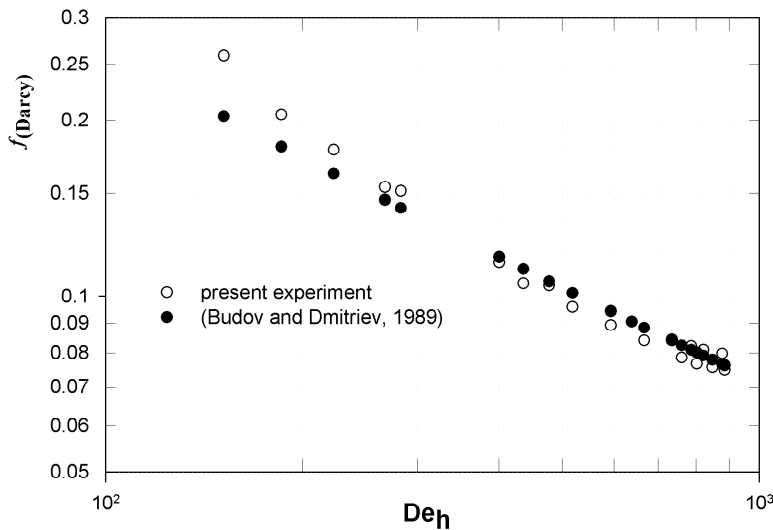
Fig. 12. Dependence of the friction factor (Darcy) on the Dean number (based on the hydraulic diameter) (EA3 case).

50
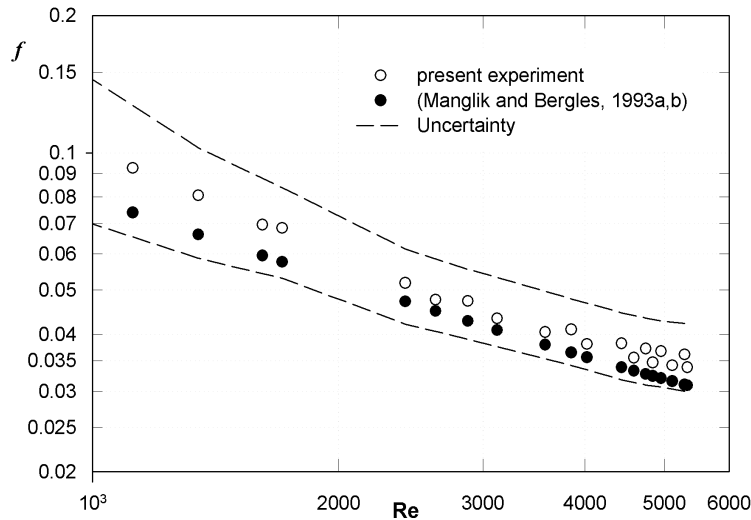
Fig. 13. Dependence of the friction factor (Fanning) on Re (EA3 case).

4.2 Thermalhydraulic characteristics of the combined inserts (integral values)

Mean convective heat transfer

The experimental results of the convective heat transfer for the combined turbulator, obtained by the EA1 and EA2 tests facilities, are presented as the function of the Re number in **Figs. 14 - 20**. The experimental data by Zimparov (2002), that concerned the combined apply of the corrugated tubes and the twisted tape, the results obtained from the calculation by Eq. (9) for the pure twisted tape at different *y* as well as the results obtained by Eq. (3) for the pure rough tubes are also presented on these charts. Here, at calculation of the Nu number by Eq. (3), the geometrical parameters of the internal tube roughness corresponded to the ones for the external ribbon of the combined turbulator as well as the helix angle of the external ribbon were calculated without taking into account the presence of the internal twisted tape. Unfortunately, due to the technical restrictions and features of the given full-scale experimental apparatus, the obtained experimental data are within a narrow range of the Re number, and in some cases this range is not even overlapped due to the different applied fuels, namely a light oil or the wood pellets.

One can see from **Figs. 14 - 20** that the heat transfer coefficients for all the studied combined turbulator inserts are generally larger than for the pure rough tube or the pure twisted-tape case. Certainly, the comparison of the combined

51

turbulator and the pure twisted tape in view of the spiral tape, considered as the basis of the combined insert, is not absolutely accurate to perform, since the width of the internal spiral tape of the combined turbulator is not the same as compared with the width of the channel itself (see **Fig. 3b**). As Al-Fahed & Chakroun (1996) have shown, the increase of a clearance between the twisted tape and the internal wall of the tube resulted in the reduction of the heat transfer.
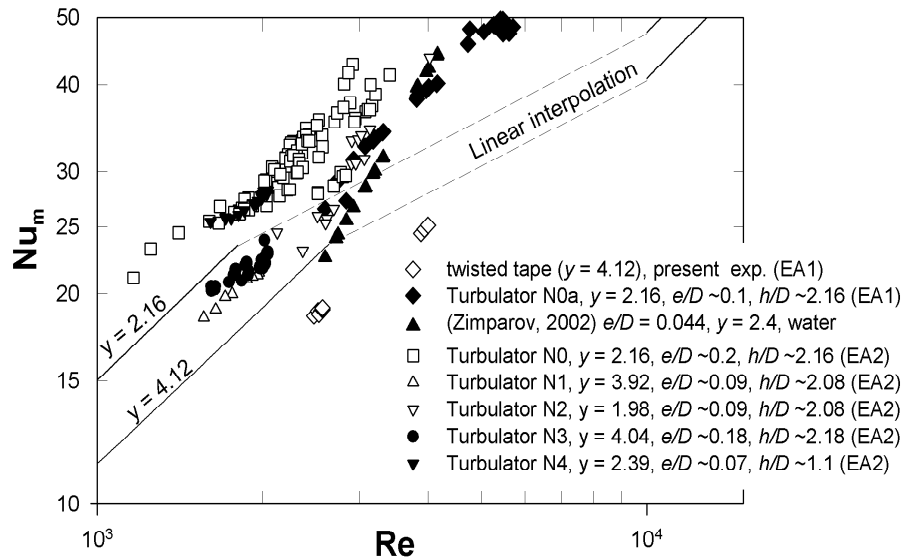
Fig. 14. The results of the convective heat transfer for the combined turbulators

It is also obvious that in order to perform the correct comparison of the combined insert and the pure rough tube, whose heat transfer characteristics are expressed by Eq. 3, the helix angle of ribbing should take into account the presence of the twisted tape. Nevertheless, the appropriate calculations with taking into account the above-mentioned consideration, show that the effect of the heat transfer enhancement is still meaningful.

The slope of the experimental curves is practically the same for all the turbulizers (N0a, N0, N1, N2, N3, N4), and it is very close to the one demonstrated by the pure twisted tape in the present research and also to the values obtained by Eq. (9) for the laminar flow regime and by Eq. (3). But, at the same time, it is smaller as compared with the data by Zimparov (2002).

As follows from the comparison of the inserts N0 and N4, there is no observable difference in the heat transfer enhancement for the approximately same twist ratio of the internal tape $y \approx 2.2$ and the twofold reduction of the relative pitch and height of the external ribbon. The twofold increase of the twist ratio of the internal twisted tape y (from ~2 up to ~4) (the inserts N1 and N2 are under consideration) for $e/D \approx 0.09$ and other geometric characteristics

52

being constant, also do not results in a significant change of the Nu number. Such behaviour is in agreement with the results by Zimparov (2002), that did not show any noticeable change of the Nu number for the smaller values of the Re number at the increase of y approximately from 2 up to 4; the relative height of the ribs after knurling was $e/D \approx 0.04$, whereas at $e/D \approx 0.2$ the approximately twofold increase of y (see N0 and N3 inserts) results in the decrease of the heat transfer.
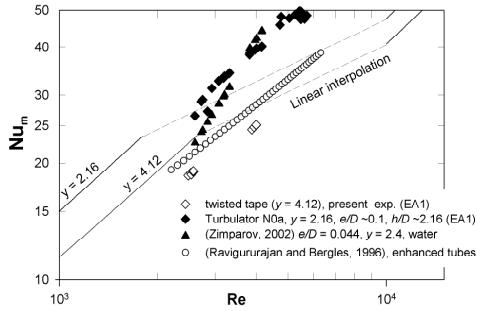
Fig. 15. The heat transfer of N0a insert
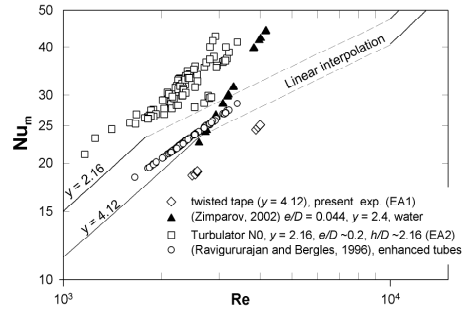
Fig. 16. The heat transfer of N0 insert
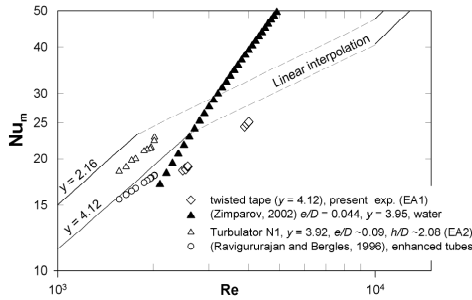
Fig. 17. The heat transfer of N1 insert
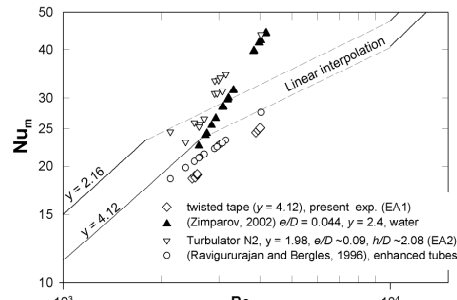
Fig. 18. The heat transfer of N2 insert
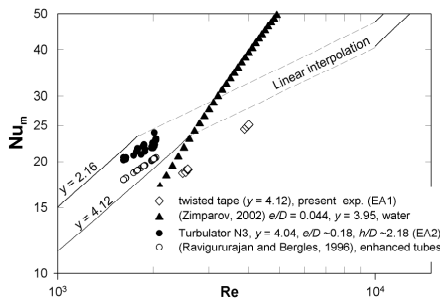
Fig. 19. The heat transfer of N3 insert
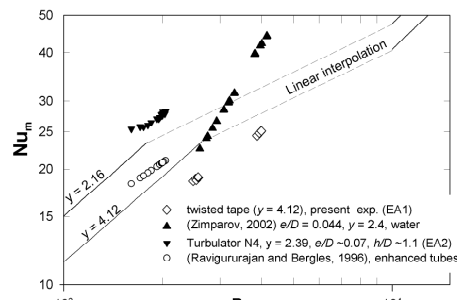
Fig. 20. The heat transfer of N4 insert

53

Here, it should be noted that for reasons of geometry only follows that the sharp angle, formed between the mean twisted flow and the external twisted tape and calculated via the envelope diameter of the tube, remains constant for inserts N0a, N0, N1, N2 and N3 for the different of y.

The increasing of the relative height of the external ribbon approximately twice at a constancy of other geometrical parameters (N0 and N0a) for $y \approx 2.16$ results in the substantial increase of Nu, while for $y \approx 4$ (N1 and N3) any increase of the Nu number was not observed.

Also, as follows from the given charts, the fairly good agreement of the experimental data obtained by the applying of the different experimental test facilities (EA1 and EA2) for inserts N0a and N2 and having roughly identical geometrical parameters, is achieved.

Fig. 21 shows the mean values of Nu_m, which were obtained by the numerical simulation, performed under the described above mathematical formulation. One can see that the satisfactory agreement with the experimental data occurs in case of the calculation for the bulk gas temperature $T_b = 573$ K (the minimum temperature that applied during the numerical tests). The values of Nu_m, calculated for the greater T_b, are either larger than the experimental ones (the runs at $T_b = 673$ K) or less them (the runs at $T_b = 873$ K).
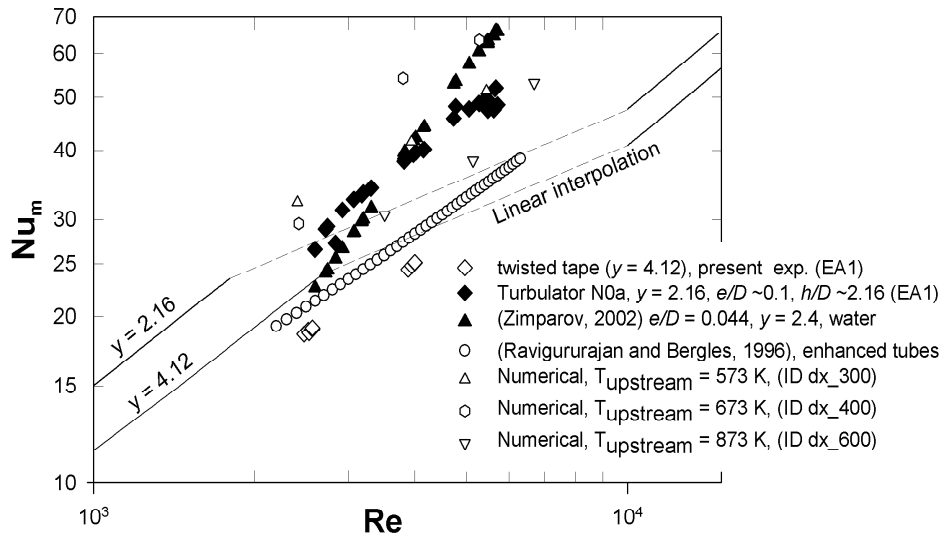
Fig. 21. The numerical results of the convective heat transfer for the combined turbulators

Pressure drop characteristics
The experimental investigation of the mean pressure drop characteristics of the combined inserts N1, N2, N3 and N4 was carried out only in the isothermal

conditions at the EA3 test facility. These results as well as the results of the numerical simulation (the integral values) that concern the runs under the isothermal and diabatic conditions, are shown in **Figs. 22 - 27**.

As it was to be expected, generally, the friction factor was substantially greater in case of the combined insert than for the individual devices (the twisted tape or the internal ribbing). The comparison of the combined inserts shows that the behaviour of the mean friction factors of all four considered inserts N1, N2, N3, N4 differs from the behaviour of the heat transfer. There were not the same values of f over all the considered range of the Re number. The largest values of the pressure drop were shown by the insert N4 and the smallest ones occurred for N1. As the Re number increases the friction factor reduces, and the slope of the curves is close to the appropriate ones taken place for the pure ribbed surface (see Eq. (3)), and it is smaller than for the pure twisted-tape case.

As also follows from **Figs. 14** and **22**, the insert having the greatest friction factor, namely N4, showed the largest heat transfer enhancement. At the same time, the inserts N1, N2 and N3, having the same heat transfer augmentation, have shown the appreciably different values of the friction factor. The greatest friction factor took place for the turbulator, which had the largest relative height of the external helix ribbon (N3, N1) at $y \approx 4$. It should be also noted that the increase of y from 2 up to 4 (the N1 and N2 inserts are intended) resulted in the increase of f for other roughly equal geometrical parameters, but the given increment was a little bit smaller than for the pure twisted-tape case (see **Fig. 22**).
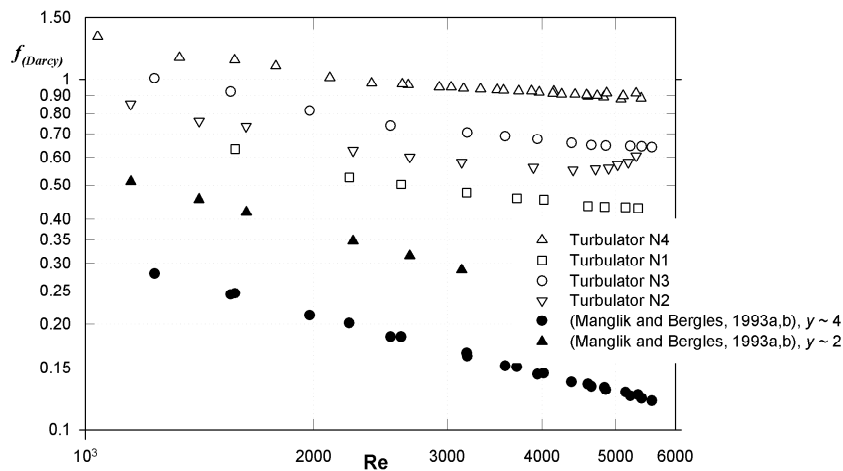
Fig. 22. The isothermal friction factor of twisted tape and combined turbulators

55
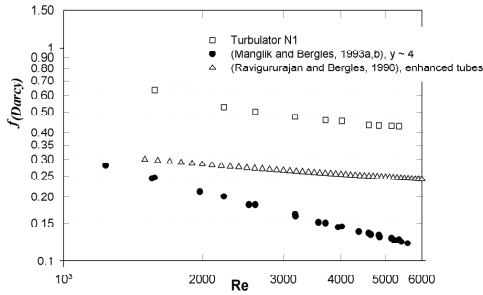
Fig. 23. The isothermal friction factor of turbulator N1
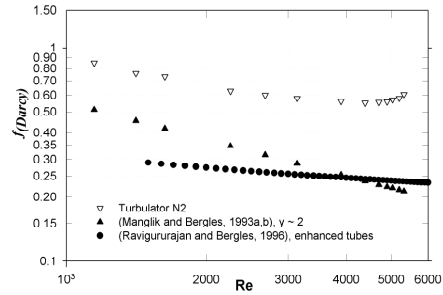
Fig. 24. The isothermal friction factor of turbulator N2
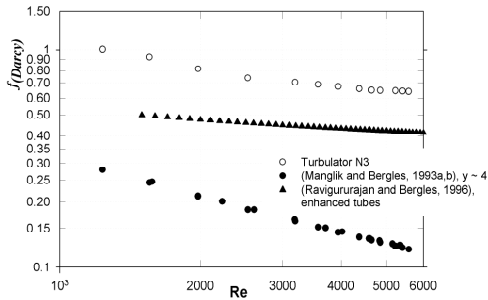
Fig. 25. The isothermal friction factor of turbulator N3
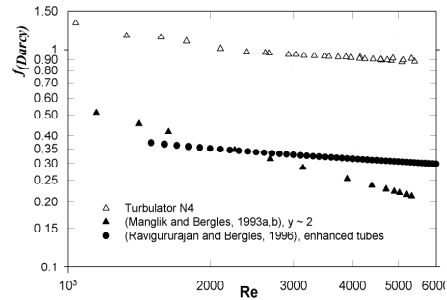
Fig. 26. The isothermal friction factor of turbulator N4
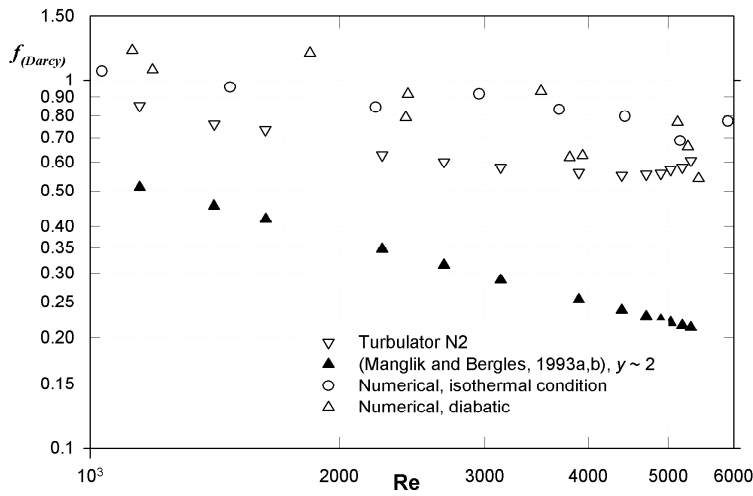
Fig. 27. The numerical results of the isothermal friction factor for the combined turbulators

56

4.3 Local thermalhydraulic characteristics of the combined insert N0a and flow structure

flow structure

Figs. 28 - 35 show the velocity vectors of the mean flow in the tube involving the combined insert, obtained by the numerical simulation in four various cross-sections (ZY plane, the flow is directed towards a viewer) of the computational domain at Re ~ 1034 and Re ~ 5906 for the isothermal conditions. These figures distinctly show the presence of the large-scale eddies, which located near the lower part of the internal twisted tape at the opposite side of the external ribbon relative to the rib. The rotating sense of these eddies is the opposite with respect to the direction of swirling of the twisted tape. One can also observe the overflows of fluid within the gap, which is formed by the twisted tape and the tube wall. The intensity of these overflows generally depends on the positional relationship of the external and the internal tapes in the given cross-section. Such flow pattern was revealed for all the investigated flow regimes both at the isothermal conditions and the presence of the heat convection.

local thermalhydraulic characteristics

Figs. 36, 37 show the distributions of the wall shear stress, circumferentially averaged over the internal surface of the tube, and the Nu number depending on the longitudinal tube coordinate X in the given cross-section (plane YZ), respectively. One can see that in both cases these distributions have periodic nature.

The wall shear stress curve at the smaller Re number (Re ~ 1034, i.e. the isothermal conditions take place) has the form of sinusoid, which transforms to a more complex curve as the Re number increases. The situation occurred in those cross-sections, where the maximum or the minimum of the wall shear stress is observed for Re ~ 1034, is not always the same as for Re ~ 3691 or ~5906. Moreover, the maximum may be changed by the minimum as the Re number increases.

The behaviour of the wall shear stress distributions in case of the isothermal conditions at Re ~ 3691 and Re ~ 5906 and behaviour of the Nu number distribution in case of the diabatic conditions, that are characterized in addition by the larger values of the fluid velocity as compared with the isothermal conditions, remains the similar depending on Re for all the discovered values of Re. One can see that the curves of distributions of the wall shear stress and the Nu number have some similarity, though the cross-sections, where the maximum or the minimum occur, may not somewhat coincide. It is also evident that the initially weak peaks of these curves rise as the Re number increases.

Figs. 38, 40 - 42 show the local circumferential distributions of the wall shear stress and the Nu number on the internal tube wall in the different cross-sections of the tube (YZ plane). These curves are plotted depending on the angle formed by the counter-clockwise turning of the unit vector OZ relative to the OZ axis (the positive direction) and expressed in degrees.

Fig. 38 presents the distribution of the local values of the wall shear stress for the adiabatic conditions at Re ~ 1034 in three various cross-sections (YZ plane), corresponding to the computational domain inlet (X = 0 m), and further to the cross-sections, where the maximum (X = 0.0175 m) and the minimum (X = 0.0375 m) of the circumferential mean values of the wall shear stress (see **Fig. 36**) were observed, respectively. It is evident that the given distribution is strongly non-uniform, and several pronounced peaks take place, that indicates the non-uniformity of distribution of the fluid mean velocity occurred over the cross-section. Generally, the number of peaks remains almost the same from one cross-section to another; their geometrical parameters (width and height) and the radial position vary only. The streamlines of the mean flow plotted for the same cross-sections (see **Fig. 39**) obviously demonstrate the behaviour of the local wall shear stress distribution.

Let us consider in more detail also the minimum (the cross-section X = 0.0175 m) and the maximum (the cross-section X = 0.0375 m) of the circumferential distributions of the mean wall shear stress along the tube at Re ~ 5906 (see **Fig. 36**). The appropriate curves of the local values of the wall shear stress in the corresponding cross-sections are shown in **Fig. 40**. These curves show that the minimum of the circumferential mean value, occurred at X = 0.0175 m, seemingly, is caused by the presence of intersection of the external and internal tapes, that takes place in the given cross-section (see also **Fig. 39**), while in the cross-section, where the maximum of the circumferential mean wall shear stress takes place, the external ribbon is located nearly at the maximum distance from the internal twisted tape. It should be noted that the same behaviour also takes place for Re ~ 3691 (see **Fig. 41**), although it is less pronounced. At the same time, the situation is quite opposite for Re ~ 1034.

The distributions of the local Nu number in the cross-sections, where the minimal (X = 0.0225 m) and the maximum (X = 0.0325 m) circumferential mean values take place (see **Fig. 37**), respectively, are plotted in **Fig. 42** for Re ~ 5440. One can see that the maximum of the circumferential mean value is seemingly conditioned by the changing towards the increase of the peak located between the angles 270° and 300 °. Here, as in case of the wall shear stress, the maximum circumferential mean value is achieved when the external ribbon is located at the maximum distance from the internal twisted tape.
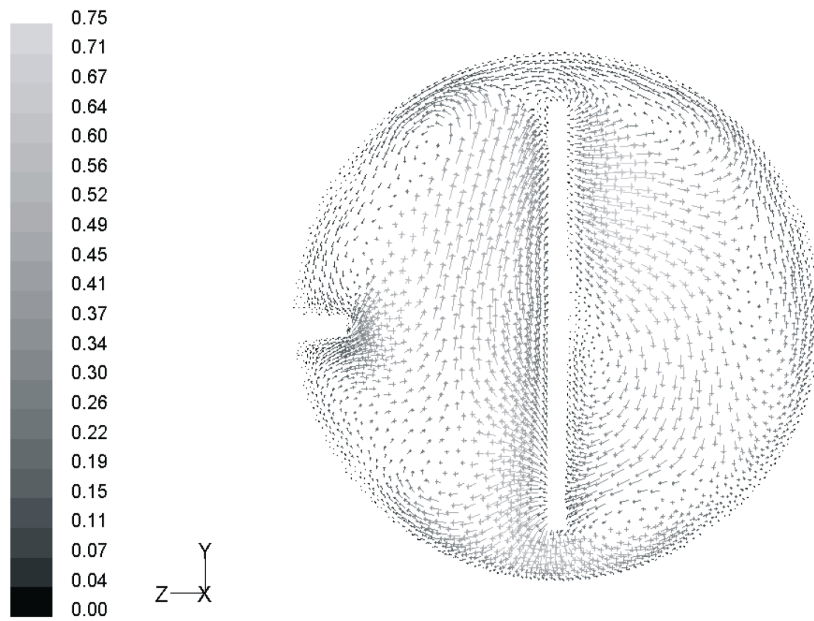
Fig. 28. The velocity distribution (m/s) at Re ≈ 1033 at the inlet (adiabatic conditions). The flow is directed towards a viewer.
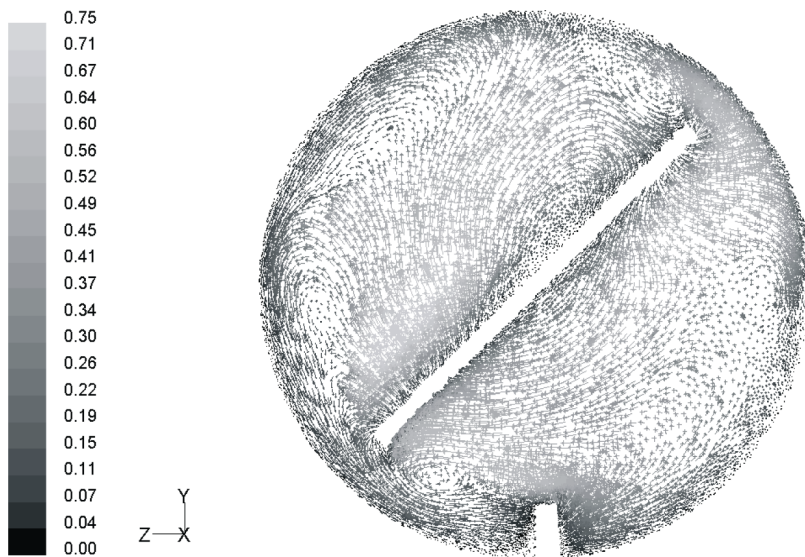
Fig. 29. The velocity distribution (m/s) at Re ≈ 1033 on Z-Y plane at X=0.025 m (adiabatic conditions) . The flow is directed towards a viewer.

59
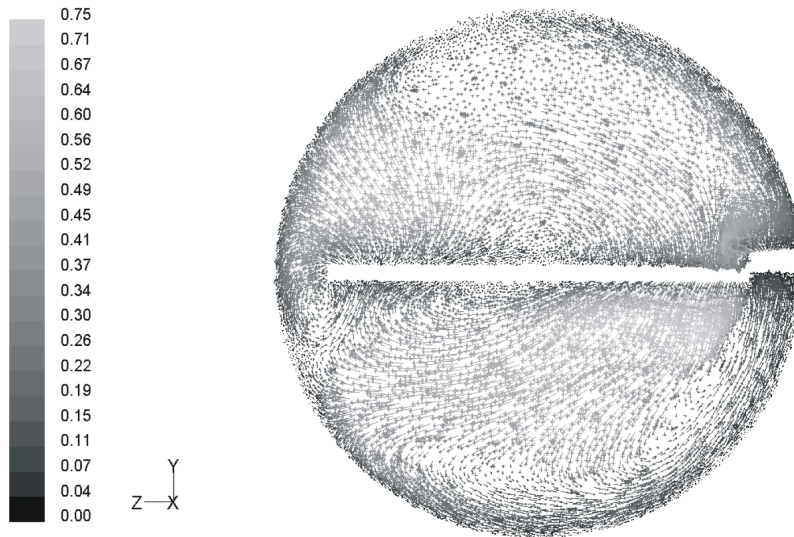
Fig. 30. The velocity distribution (m/s) at Re ≈ 1033 on Z-Y plane at X=0.05 m (adiabatic conditions). The flow is directed towards a viewer.
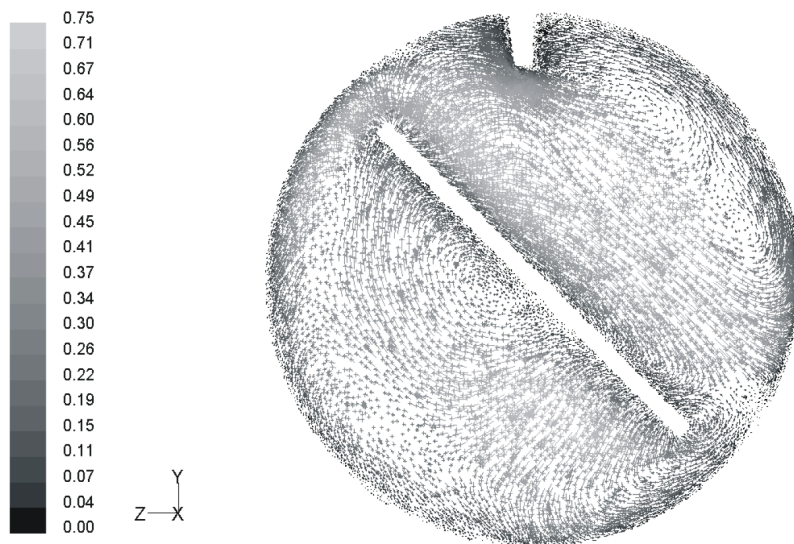
Fig. 31. The velocity distribution (m/s) at Re ≈ 1033 on Z-Y plane at X=0.075 m (adiabatic conditions). The flow is directed towards a viewer.
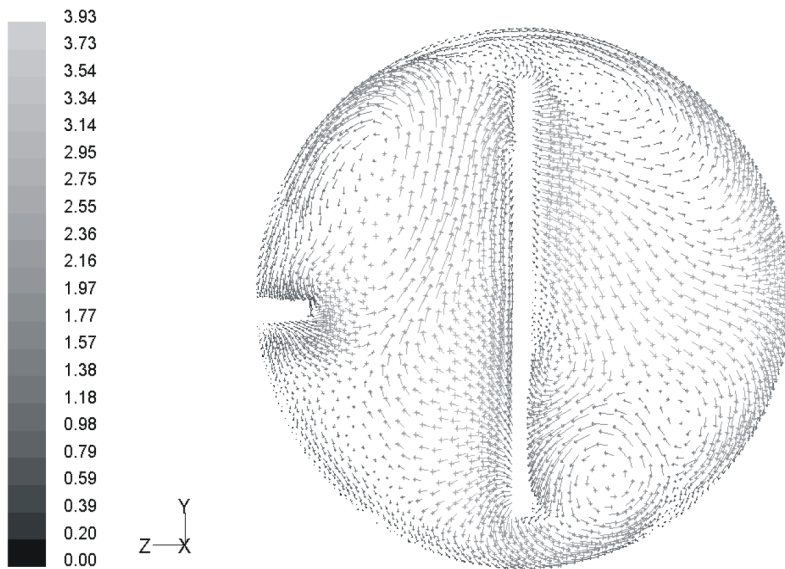
Fig. 32. The velocity distribution (m/s) at Re ≈ 5906 on inlet (adiabatic conditions). The flow is directed towards a viewer.
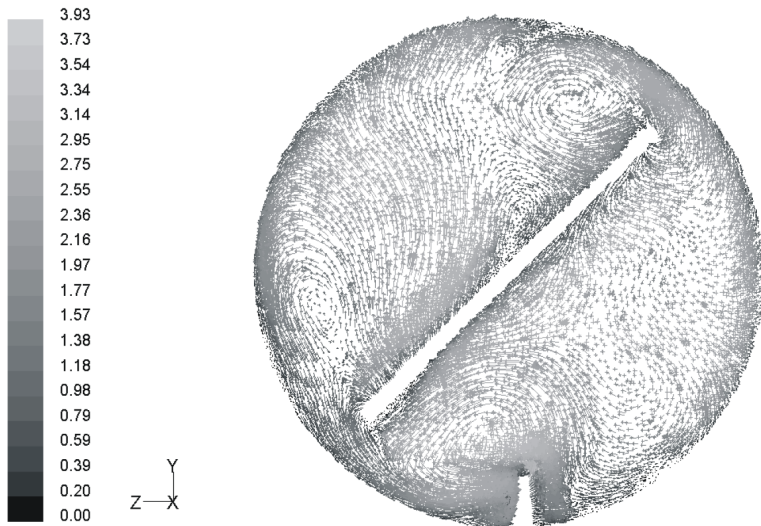
Fig. 33. The velocity distribution (m/s) at Re ≈ 5906 on Y-Z plane at X = 0.025 m(adiabatic conditions). The flow is directed towards a viewer.

61
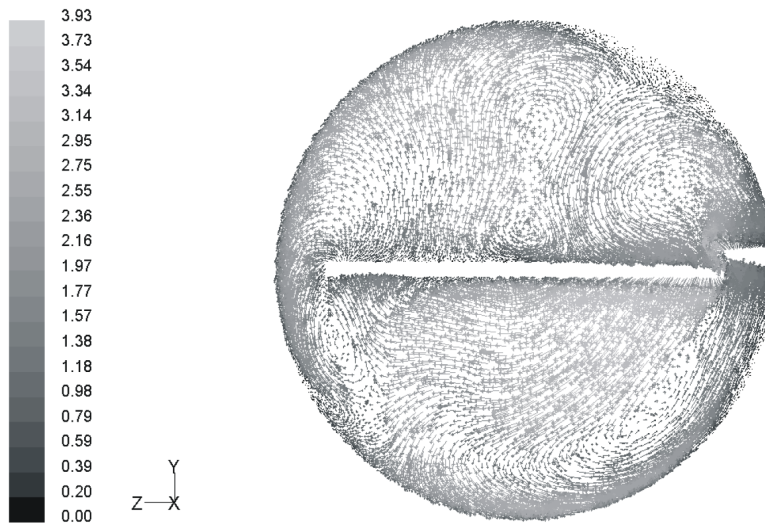
Fig. 34. The velocity distribution (m/s) at Re ≈ 5906 on Y-Z plane at X = 0.05 m (adiabatic conditions). The flow is directed towards a viewer.
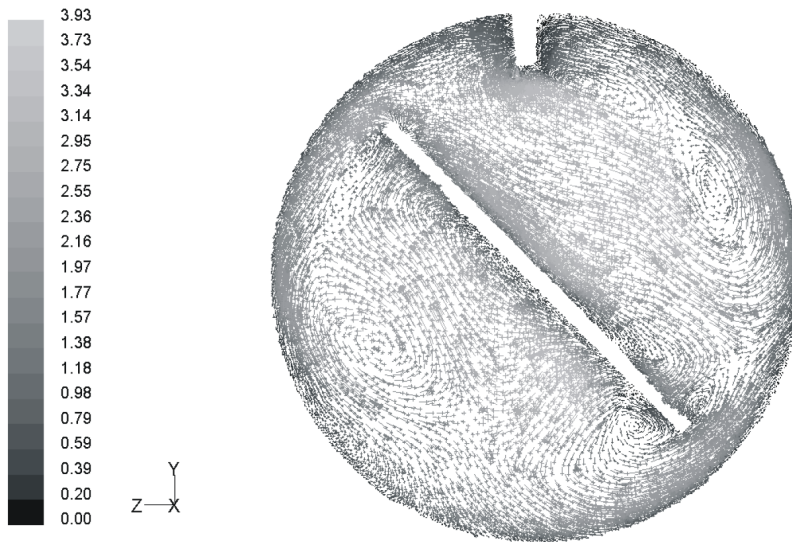
Fig. 35. The velocity distribution (m/s) at Re ≈ 5906 on Y-Z plane at X = 0.075 m (adiabatic conditions). The flow is directed towards a viewer.
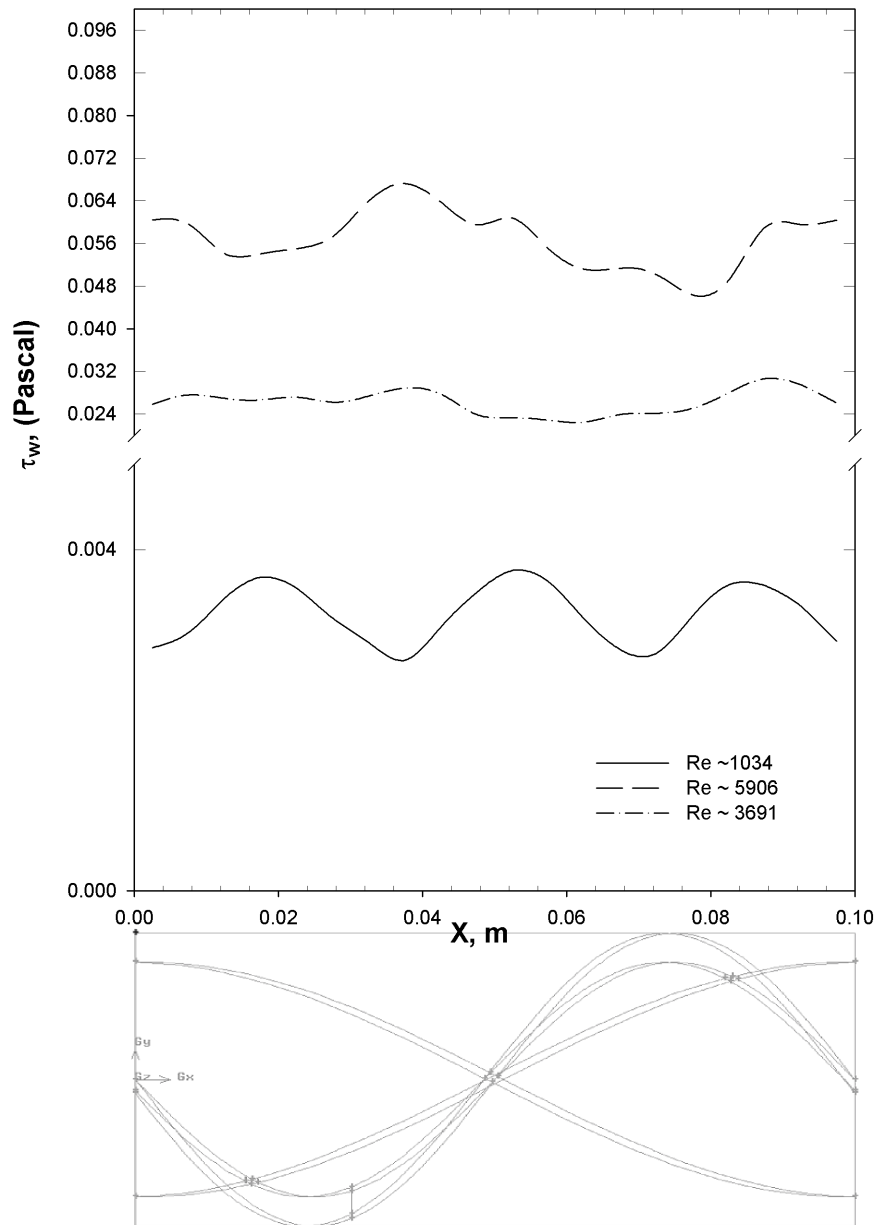
Fig. 36. The distribution of the circumferential mean values of the wall shear stress on a tube wall along X axis (adiabatic conditions)
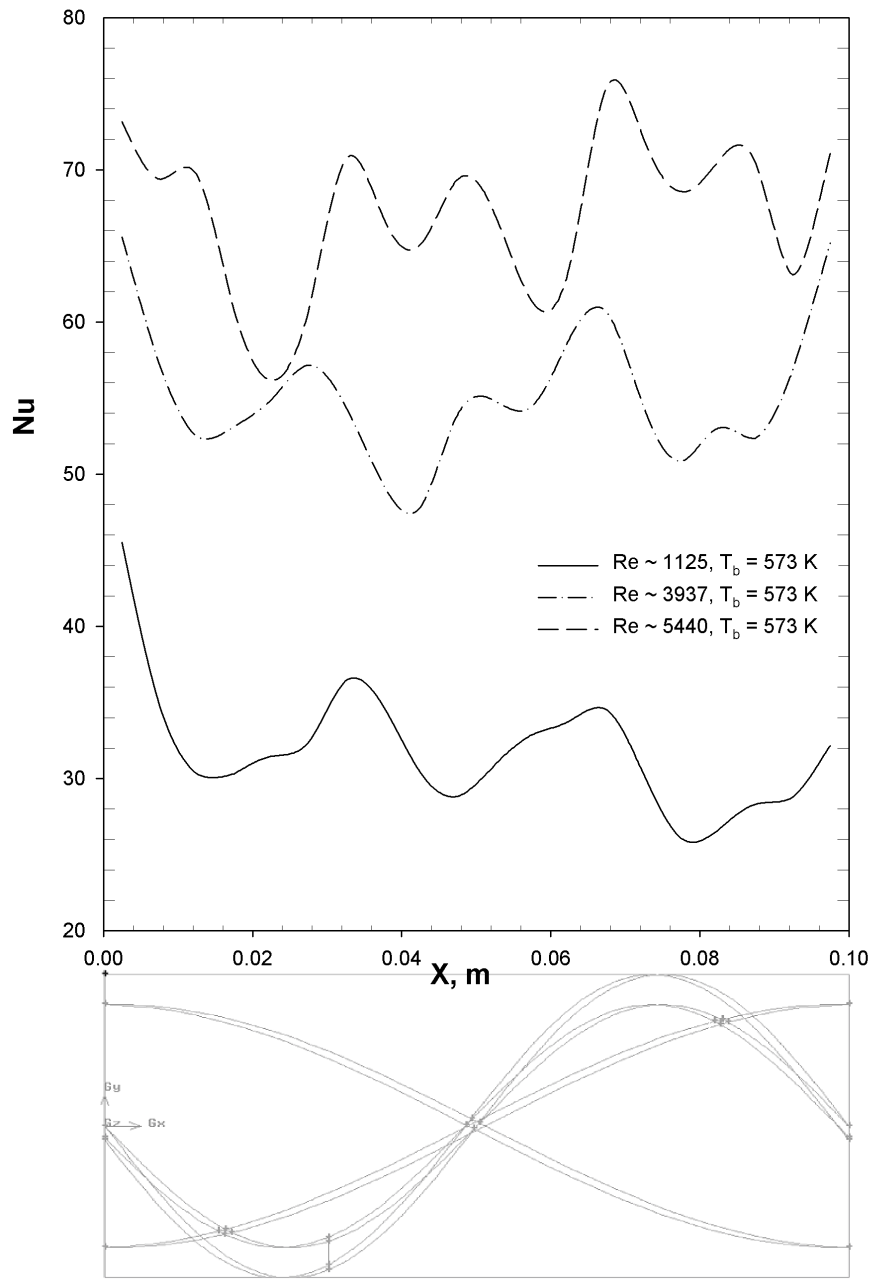
Fig. 37. The distribution of the circumferential mean values of Nu on a tube wall along X axis.
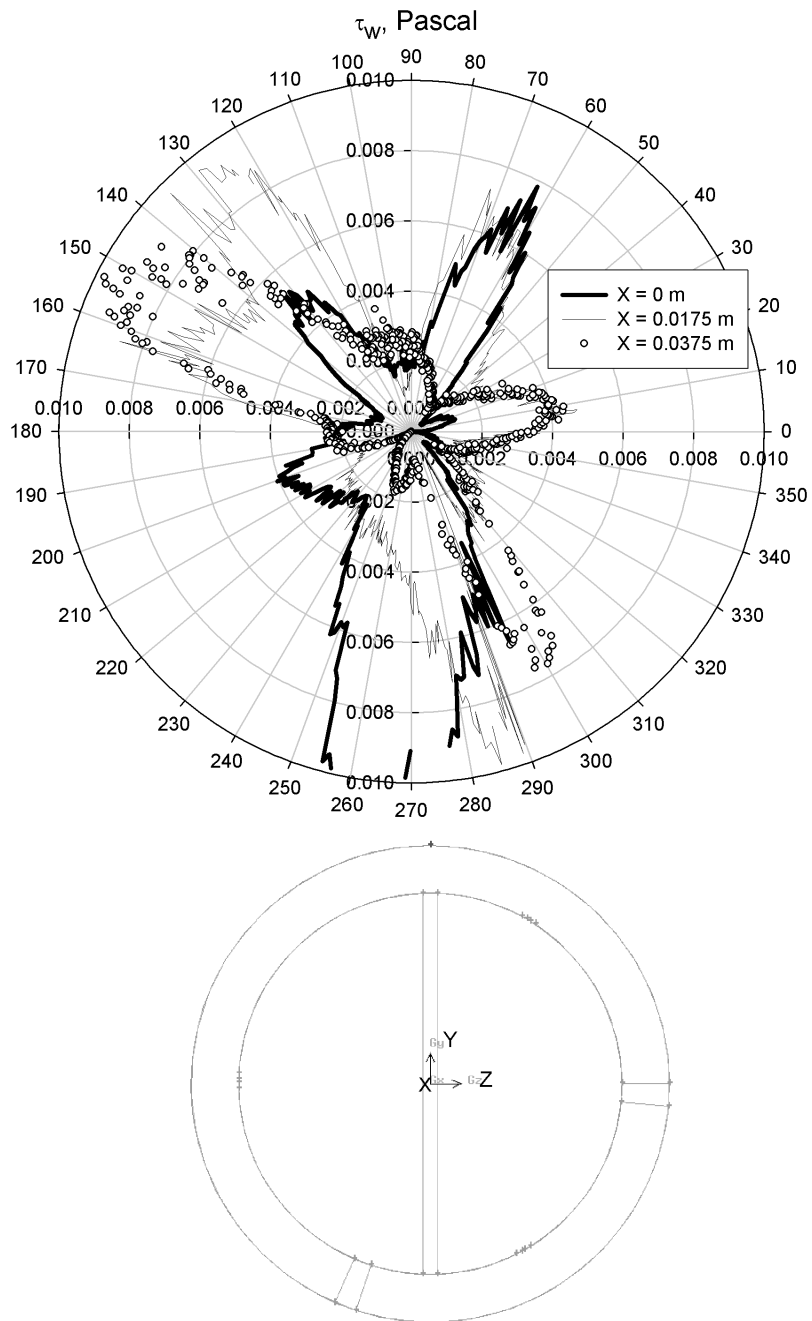
Fig. 38. The wall shear stress distribution at the internal surface of a tube at three different cross-sections (Re ~ 1034, adiabatic conditions).

X = 0 m

X = 0.0175 m

Y

X   Z

X = 0.0375 m
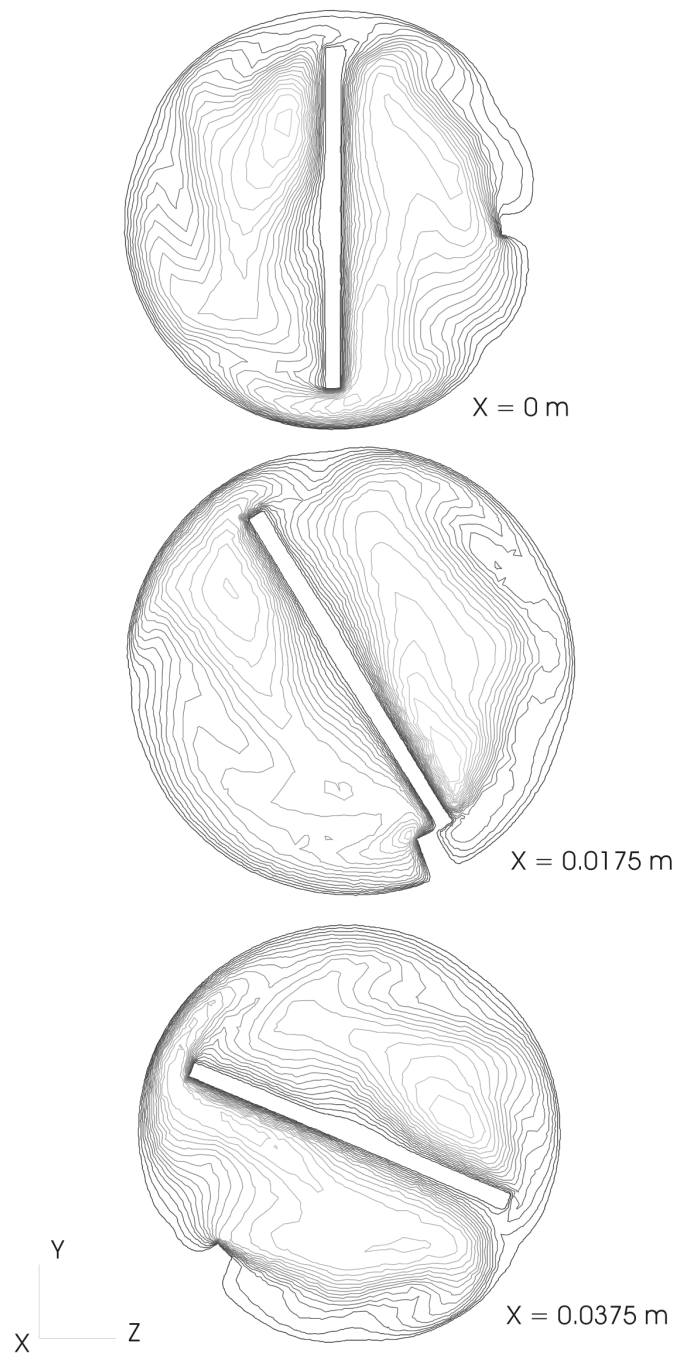
**Fig. 39. The flow stream lines at three different cross-sections of a tube
(Re ~ 1034, adiabatic conditions).**
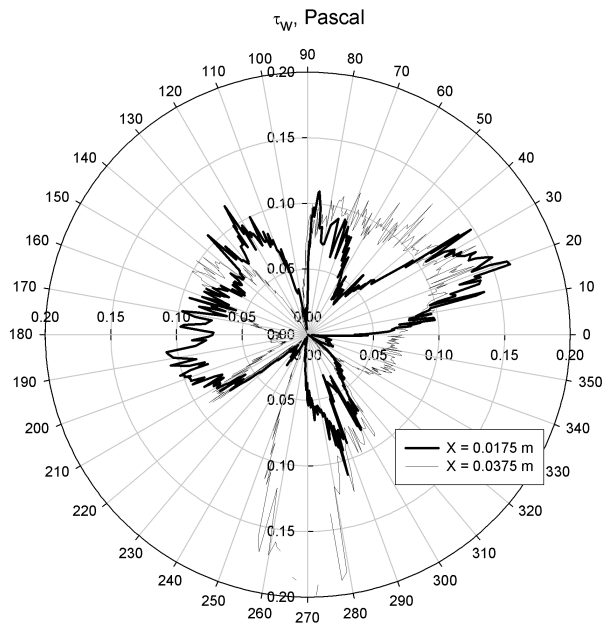
Fig. 40. The wall shear stress distribution at the internal surface of a tube at two different cross-sections (Re ~ 5906, adiabatic conditions).
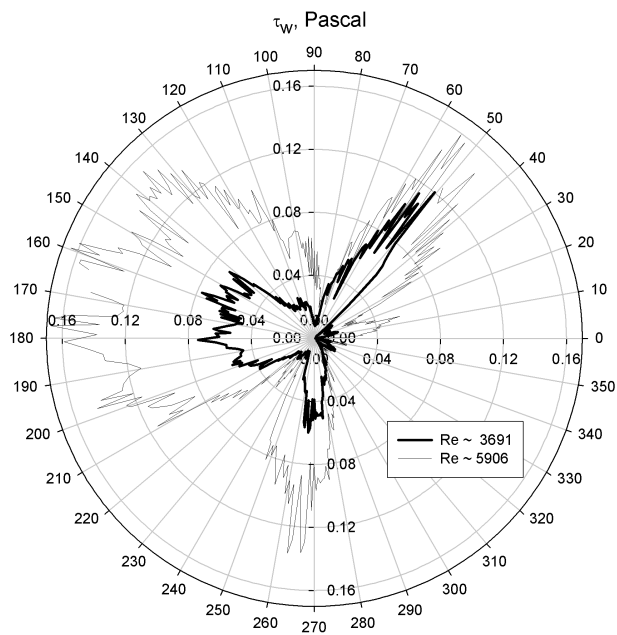
Fig. 41. The wall shear stress distribution at the internal surface of a tube for two different Re at the cross-section X = 0 m (adiabatic conditions).

67
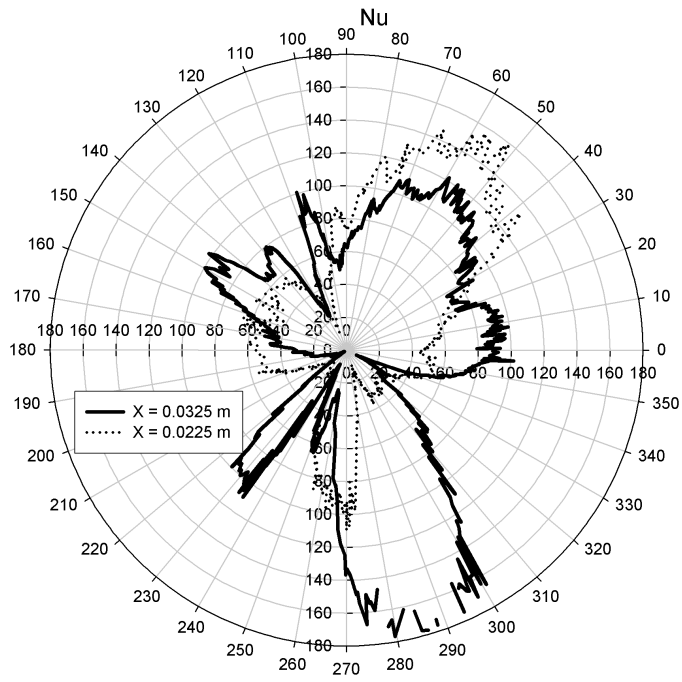
Fig. 42. The distribution of the local Nu at the internal surface of a tube at two different cross-sections (Re ~ 5440).

5. SOME CONSIDERATIONS FOR CORRELATION DEVELOPMENT AND FURTHER RESEARCH

Unfortunately, the obtained experimental data are not enough to derive the reliable correlations for the prediction of the heat transfer coefficients and the friction factors depending on various geometrical parameters of the considered inserts.

Nevertheless, the qualitative analysis of the flow pattern, performed during the numerical simulation, has shown its similarity to the case of the applying of the pure twisted tape. During this analysis the presence of the overflows of fluid, occurred in the gap between the twisted tape and the tube wall and influenced additionally on the heat transfer and the pressure drop, was also revealed. Therefore, it is quite reasonable to suppose, that the heat transfer coefficients and the friction factors taken place in case of the combined use of the internally spirally ribbing tubes and the twisted tape, may be correlated similarly to the case of the pure twisted tape as follows:

$$\frac{f_{combined}}{f_{rib}}, \frac{Nu_{combined}}{Nu_{rib}} = \Phi(y,k), \tag{44}$$

where k is the variable, which characterize the influence of the gap, taken place between the internal twisted tape and the tube wall, on the friction factor or the heat transfer. Here, it is assumed that the flow is the fully developed turbulent flow with Re > 10000.

The numerator of Eq. (44) contains the values of Nu and f, that corresponds to the case of the combined insert, and the denominator includes the values of Nu and f for the ribbed surface, taking into account the change of the attack angle of the mean flow relative to the ribs, caused by the additional installation of the twisted tape. The given attack angle can be expressed by the following formula:

$$\beta = 180° - (\alpha_{rib} + \alpha_{twiste-tape}). \tag{45}$$

The assumptions, stated in the given thesis, have been validated based on the analysis of the experimental data by Zimparov (2002), obtained for the fully developed turbulent flow with Re > 10000. The given analysis was performed as follows. The prediction by Eq. (2) and (3) was generally used for the calculation of Nu_{rib} and f_{rib} included in the denominator of Eq. (44). Here it should be noted that these correlations with high accuracy describe the experimental data obtained by Zimparov (2002) for the corrugated tubes. The difference for f is less than 10 %, and for the Nu number the maximum difference is less than 25 %. Here the calculation of Nu_{rib} by Eq. (44) takes into account the difference between the slopes of curves, plotted in the coordinate frame Nu vs. Re, which were obtained by Zimparov (2002) and by Eq. (3). The validation on the basis of the above described approach allowed to achieve a good agreement with the assumptions, which were made hereinbefore. However, these assumptions are in need of more accurate verification by means of the further investigations.

CONCLUSIONS

The given thesis is dedicated to the experimental and numerical investigations concerning the proposed technique for the heat transfer intensification in the convective part of the fire-tube boilers.

The integral values of the total and the convective heat transfer for the combined heat transfer intensifying inserts of various geometrical parameters have been obtained experimentally during the full-scale tests. The hydraulic characteristics of the inserts have been studied for the isothermal conditions with the help of the experimental set-up, which had been designed and constructed by the author of the given thesis. A satisfactory qualitative agreement has been achieved with the results, obtained by the full-scale experimental set-up. The significant increase of the heat transfer coefficients (up to ~50 %) has been obtained as compared with the pure twisted tape at simultaneous faster rise of the pressure drop.

The additional investigations of the smooth tube, straight and twisted tape have been performed for the validation of the obtained experimental results.

The three-dimensional numerical simulation has been carried out for the fully developed flow by means of the RNG κ–ε turbulence model with the applying of the FLUENT CFD code. The numerical simulation covered the total range of the flow regimes observed in the experimental part of the given thesis. The simulation was performed for the combined insert, which was identical to the one applied in the horizontal channel during the full-scale tests. The computed integral values of the convective heat transfer coefficients and the friction factors have shown a good agreement with the experimental data. The obtained local longitudinal and circumferential distributions of the heat transfer coefficients and the wall shear stress on the internal surface of the tube have shown their periodic nature.

Based on the analysis of the flow pattern in a tube in presence of the combined insert as well as the experimental data by Zimparov (2002), the method for the prediction of the heat transfer coefficients and the friction factors have been elaborated for the fully developed turbulent flow regime.

70

REFERENCES

Aicher, T., Martin, H. 1997. New correlations for mixed turbulent natural and forced convection heat transfer in vertical tubes, Int. J. Heat Mass Transfer, Vol. 40, No. 15, pp. 3617-3626.

Al-Fahed, S., Chakroun, W. 1996. Effect of tube-tape clearance on heat transfer for fully developed turbulent flow in a horizontal isothermal tube, Int. J. Heat and Fluid Flow 17, pp. 173-178.

Ambrazevičius, A. 2003. High temperature heat transfer for subsonic diatomic gaseous flows in tubes. pp. 293-300., In: Advances of Heat Transfer Engineering (Proc. of 4th BHTC, Kaunas, Aug. 25-27, 2003). Ed. by B. Sunden and J. Vilemas.

Bergles, A. E. 2002**.** ExHFT for fourth generation heat transfer technology, Experimental Thermal and Fluid Science 26, pp. 335-344.

Bergles, A. E., Lee, R. A., Mikic, B. B. 1969. Heat Transfer in Rough Tubes with Tape-Generated Swirl Flow. Trans. ASME, J. Heat Transfer 91, pp. 443-445.

Bohne, D., Obermeier, E. 1986. Combined free and forced convection in a vertical and inclined cylindrical annulus, Proc. 8th Intern. Heat Transfer Conference, San Francisco, CA U.S.A., Vol. 3, pp. 1401-1406.

Budov, V. M., Dmitriev, S. M. 1989. Forced Heat Exchangers of NPS (nuclear power system). (Forsirovanniye teploobmenniki YaEU). Moscow, Energoatomizdat, 1989 (III), (Fisika I tehnika yadernih reaktorov, Vip. 40) ISBN 5-283-03779-7.

Choudhury, D. 1993. Introduction to the Renormalization Group Method and Turbulence Modeling. Fluent Inc. Technical Memorandum TM-107, 1993.

Cui, J., Patel, V. C., Lin, C-L. 2003. Large-eddy simulation of turbulent flow in a channel with rib roughness. Int. J. of Heat and Fluid Flow, 24, pp. 372-388.

Dipprey, D. F., Sabersky, R. H. 1962. Heat and momentum transfer in smooth and rough tubes at various Prandtl numbers. Int. J. Heat Mass Transfer. Vol. 6. pp. 329-353.

Dzyubenko, B. V., Dreitser, G. A. 1994. Heat transfer intensification in channels with the artificial flow turbulization. (*Intensifikaciya teploobmena v kanalakh s iskustvennoy turbulizatsiyey potoka*). First Russian National Heat Transfer Conference (*pervaya rossiyskaya natsionalnaya konferentsiya po teploobmenu*). Izd. MEI, Moscow, Vol. VII., pp. 64-69.

Fluent 6.1 User's guide. Fluent Inc. Centerra Resource Park, 10 Cavendish Court, Lebanon, NH 03766, February 2003.

Gachechiladze, I. A., Kiknadze, G. I., *et al*. 1988. Heat Transfer with Self-Organization of Tornado Structureres, Minsk Int. Forum (MMF), *Radiative and Combined Heat Transfer: Problem Reports,* Minsk: ITMO, Sections 1, 2, pp.83-125.

Gnielinski, V. 1976. New equations for heat and mass transfer in turbulent pipe and channel flow, International chemical engineering, Vol.16, No. 2, pp. 359-368, April 1976.

Hishida, Makoto. 1996. Local Heat Transfer Coefficient Distribution on a Ribbed Surface. Journal of Enhanced Heat Transfer, Vol.3, No. 3, pp. 187-200.

Isachenko, V. P., Osipova, V. A., Sukomel, A. S. 1981. Heat Transfer (Teploperedacha). 4th Edition, Moscow, Enorgoizdat, (in Russian).

Junkhan, G. H., Bergles, A. E., Nirmalan, V., Ravigururajan, T. 1985. Investigation of Turbulators for Fire Tube Boilers. Heat Mass Transfer, Vol. 107, No. 2.

Kalinin, E. K., Dreitser, E. V., Yarkho, S. A. 1990. Intensifikatsiya Teploobmena v Kanalakh *(Enhancement of Heat Transfer in Channels)*, Mashinostroyeniye Press, Moscow, 3rd ed.

Kenji Katoh, Kwing-So Choi, Tsueneo Azuma. 2000. Heat-transfer enhancement and pressure loss by surface roughness in turbulent channel flows. Int. J. of Heat and Mass Transfer 43, pp. 4009-4017.

Kurganov, V. A. 1992. Heat transfer in turbulent gas flow in tubes, Teploenergetika, No. 5, pp. 2-9, (in Russian).

Kutateladze, S.S. 1990. Heat transfer and friction, Handbook, Energoatomizdat, Moscow, (in Russian).

Liao, Q., Xin, M. D. 2000. Augmentation of convective heat transfer inside tubes with three-dimensional internal extended surfaces and twisted-tape inserts. Chemical Engineering Journal, 78, pp. 95-105.

Lopina, R. F., Bergles, A. E. 1969. Heat Transfer and Pressure Drop in Tape-Generated Swirl Flow of Single-Phase Water. Trans. ASME, J. Heat Transfer 91, pp. 434-442.

Manglik, R. M., Bergles, A. E. 1993a. Heat transfer and pressure drop correlations for twisted-tape inserts in isothermal tubes: part I – laminar flows, Journal of Heat Transfer, Vol. 115, pp. 881-889, November 1993.

Manglik, R. M., Bergles, A. E. 1993b. Heat transfer and pressure drop correlations for twisted-tape inserts in isothermal tubes: part II – transition and turbulent flows, Journal of Heat Transfer, Vol. 115, pp. 890-896, November 1993.

Manglik, R. M., Maramraju, S., Bergles, A. E. 2001. The Scaling and Correlation of Low Reynolds Number Swirl Flows and Friction Factors in Circular Tubes with Twisted-Tape Inserts. Journal of Enhanced Heat Transfer, 8, pp. 383-395.

Migay, V. K. 1987. Modeling of the heat-transfer power equipment. (Modelirovaniye teploobmennogo energeti4eskogo oborudovaniya). Leningrad, Energoatomizdat, Leningradskoye otdeleniye.

Moffat, R. J. 1988. Describing the uncertainties in experimental results, Experimental Thermal and Fluid Science, 1, pp. 3-17.

Nagano, Y., Hattori, H., Houra, T. 2004. DNS of velocity and thermal fields in turbulent channel flow with transverse-rib roughness. Int. J. of Heat and Fluid Flow, 25, pp. 393-403.

Neshumajev, D., Tiikma, T., Träss, O. 1999. Effects of surface with regular roughness on convective heat transfer. Progress in Engineering Heat Transfer.

Ed. B. Grochal, J. Mikielewicz, B. Sunden. (Proc. of 3rd Baltic Heat Transfer Conference). IFFM Publishers, Gdansk,. pp. 407 – 414.

Neshumayev D., Ots A., Laid J., Tiikma T. 2003. Heat transfer augmentation and pressure drop of turbulator inserts in gas-heated channels, pp. 565-572. In: Advances of Heat Transfer Engineering (Proc. of 4th BHTC, Kaunas, Aug. 25-27, 2003). Ed. by B. Sunden and J. Vilemas.

Patankar, S. V., Liu, C. H., Sparrow, E. M. 1977. Fully Developed Flow and Heat Transfer in Ducts Having Streamwise-Periodic Variations of Cross-Sectional Area. ASME J. Heat Transfer, Vol. 99, pp. 180-186.

Pedišius, A., Šlančiauskas, A. 1995. Heat Transfer Augmentation in Turbulent Flows, Lithuanian Energy Institute and Begell House, New York – Kaunas.

Petukhov, B. S. 1970. Heat transfer and friction in turbulent pipe flow with variable physical properties, Advances in Heat Transfer, Vol. 6, Academic Press, New York, pp. 503-564.

Petukhov, B. S., Polyakov, A. F. 1986. Heat transfer in turbulent mixed convection, Nauka, Moscow, (in Russian).

Ravigururajan, T. S., Bergles, A. E. 1996. Development and Verification of General Correlations for Pressure Drop and Heat Transfer in Single-Phase Turbulent Flow in Enhanced Tubes. Experimental Thermal and Fluid Science, 13, pp. 55-70.

Repik, E. U., Kuzenkov, V. K. 1989. Accuracy of static pressure measurements depending on drain ports. (Pogreshnosti izmereniya stati4eskogo davleniya pri ispolzovanii drenaznih otverstiy). IFZh, Vol. 57, No. 6, December.

Repik, E. U., Kuzenkov, V. K. 1990. Measurements of static pressure with drain ports with minimum accuracy. (Izmereniye stati4eskogo davleniya s pomoshchyu drenaznih otverstiy s minimalnoy pogreshnostyu). IFZh, Vol. 59, No. 2.

Smithberg, E., Landis, F. 1964. Friction and Forced Convection Heat-Transfer Characteristics in Tubes with Twisted Tape Swirl Generators. Trans. ASME, J. Heat Transfer 86, series C, No. 1.

Spalding, D. B., Taborek, J. 1983. Heat exchanger design handbook, Hemisphere Publishing Corporation.

Tamonis, M. 1981. Radiation and combined heat transfer in channels, VILNIUS, "MOKSLAS", (in Russian).

Usui, H, Sano, Y., Iwashita, K., Isozaki, A. 1986. Enhancement of heat transfer by a combination of an internally grooved rough tube and a twisted tape. INTERNATIONAL CHEMICAL ENGINEERING, Vol. 26, No 1, pp. 97-104.

Van Rooyen, R. S., and Kröger, D. G. 1978. Laminar Flow Heat Transfer in Internally Finned Tubes with Twisted-Tape Inserts, in Heat Transfer 1978, Vol. 2, Hemisphere Publishing, Washington, DC, pp. 577-581.

Versteeg, H. K., Malalasekera, W. 1995. An introduction to computational fluid dynamics, Longman Group Ltd, 1995.

Vilemas, J., Šimonis, V., Adomaitis, J. E. 1989. Heat transfer augmentation in gas-cooled channels. Monograph, Editor Prof. A. Žukauskas, VILNIUS, Mokslas publ.

Wu, H., Cheng, H., Zhou, Q. 2000. Compound Enhanced Heat Transfer Inside Tubes by Combined Use of Spirally Corrugated Tubes and Inlet Axial Vane Swirlers. Enhanced Heat Transfer, Vol. 7, pp. 247-257.

Zhang, Y. M., Han, J. C. and Lee, C. P. 1997. Heat Transfer and Friction Characteristics of Turbulent Flow in Circular Tubes with Twisted-Tape Inserts and Axial Interrupted Ribs. Enhanced Heat Transfer, Vol. 4, pp. 297-308.

Zimparov, V. 2002. Enhancement of heat transfer by a combination of a single-start spirally corrugated tubes with a twisted tape, Experimental Thermal and Fluid Science 25, pp. 535-546.

Zimparov, V. 2004 Part1. Prediction of friction factors and heat transfer coefficients for turbulent flow in corrugated tubes combined with twisted tape inserts. Part 1: friction factors. Int. J. of Heat and Mass Transfer, 47, pp. 589-599.

Zimparov, V. 2004 Part2. Prediction of friction factors and heat transfer coefficients for turbulent flow in corrugated tubes combined with twisted tape inserts. Part 2: heat transfer coefficients. Int. J. of Heat and Mass Transfer, 47, pp. 385-393.

Žukauskas, A. A. 1982. Konvektivnyy perenos v teploobmennikakh (Convective heat transfer in heat exchangers), Nauka Press, Moscow, (in Russian).

ORIGINAL PUBLICATIONS

PAPER I

PAPER II

PAPER III (Utility model)

CURRICULUM VITAE

Name	Dmitri
Surname	Neshumayev
Date and place of birth	October 25, 1974, Estonia
Family status	Married
Contact	Jahu 1-3, 10415 Tallinn, Estonia,
	GSM: +37255651943
	e-mail: vladn@staff.ttu.ee
Workplace	Tallinn University of Technology,
	Thermal Engineering Department,
	Kopli 116, 11712 Tallinn, Estonia
	e-mail: vladn@staff.ttu.ee
Appointment	Research scientist

Education:

Institution [Date from - Date to]	Degree(s) or Diploma(s) obtained:
Kehra Secondary School [1991]	Secondary-level Educations
Tallinn University of Technology [1991 – 1996]	Engineer in power engineering
Tallinn University of Technology [1996 – 1998]	M.Sc., (power engineering)
Tallinn University of Technology [1999 – to present]	Ph. D. student

Work experience	since 1997, Tallinn University of Technology, Research scientist
Scientific degree	Master of Science
Certificate of education	Tallinn University of Technology, 1998
Scientific work	Heat transfer intensification by passive techniques

ELULOOKIRJELDUS (CV)

Eesnimi	Dmitri
Perekonnanimi	Nešumajev
Sünniaeg ja –koht	25. Oktoober 1974, Eesti
Perekonnaseis	Vabaabielus
Kontaktandmed	Jahu 1-3, 10415 Tallinn, Eesti,
	GSM: +37255651943
	e-mail: vladn@staff.ttu.ee
Töökoht	Tallinna Tehnikaülikool,
	Soojustehnika instituut,
	Kopli 116, 11712 Tallinn, Eesti
	e-mail: vladn@staff.ttu.ee
Ametikoht	Teadur

Hariduskäik:

Õppeasutus [aeg]	Haridus
Kehra Keskkool [1991]	keskharidus
Tallinna Tehnikaülikool [1991 – 1996]	soojusenergeetika insener
Tallinna Tehnikaülikool [1996 – 1998]	energiatehnika õppesuund/tehnikateaduste magister
Tallinna Tehnikaülikool [1999 – k.a]	doktorant

Teenistuskäik	1997 - k.a., Tallinna Tehnikaülikool,
	Soojustehnika instituut, teadur
Teaduskraad	tehnikateaduste magister
Teaduskraadi välja andnud asutus, aasta	Tallinna Tehnikaülikool, 1998
Teadustöö põhisuunad	Soojusülekande intensifitseerimine